UNIVERSIDADE ESTADUAL DE CAMPINAS

INSTITUTO DE BIOLOGIA

GRAZIELLE CELESTE MAKTURA

SARS-CoV-2 UTILIZA O FLUXO DE AUTOFAGIA INCOMPLETO PARA PROMOVER A REPLICAÇÃO VIRAL E CONEXÕES CÉLULA-CÉLULA PARA PROMOVER A EVASÃO CELULAR

SARS-CoV-2 UTILIZES INCOMPLETE AUTOPHAGY FLUX TO PROMOTE VIRAL REPLICATION AND CELL-TO-CELL CONNECTIONS TO PROMOTE CELLULAR EVASION

CAMPINAS
2023

GRAZIELLE CELESTE MAKTURA

SARS-CoV-2 UTILIZES INCOMPLETE AUTOPHAGY FLUX TO PROMOTE VIRAL REPLICATION AND CELL-TO-CELL CONNECTIONS TO PROMOTE CELLULAR EVASION

SARS-CoV-2 UTILIZA O FLUXO DE AUTOFAGIA INCOMPLETO PARA PROMOVER A REPLICAÇÃO VIRAL E CONEXÕES CÉLULA-CÉLULA PARA PROMOVER A EVASÃO CELULAR

Dissertation presented to the Institute of Biology of the State University of Campinas in partial fulfillment of the requirements for the degree of Master in Molecular and Morphofunctional Biology, in the Area of Cellular Biology.

Dissertação apresentada ao Instituto de Biologia da Universidade Estadual de Campinas como parte dos requisitos exigidos para a obtenção do título de Mestra em Biologia Molecular e Morfofuncional, na Área de Biologia Celular.

ADVISOR: PROF. DR. HENRIQUE MARQUES BARBOSA DE SOUZA

THIS DIGITAL FILE CORRESPONDS TO THE FINAL VERSION OF THE THESIS DEFENDED BY STUDENT GRAZIELLE CELESTE MAKTURA AND ADVISED BY PROF. DR. HENRIQUE MARQUES BARBOSA DE SOUZA.

CAMPINAS

2023

M289s Maktura, Grazielle Celeste, 1996-
SARS-CoV-2 utiliza o fluxo de autofagia incompleto para promover a replicação viral e conexões célula-célula para promover a evasão celular / Grazielle Celeste Maktura. – Campinas, SP : [s.n.], 2023.

Orientador: Henrique Marques Barbosa de Souza.
Dissertação (mestrado) – Universidade Estadual de Campinas, Instituto de Biologia.

1. SARS-CoV-2. 2. Células vero. 3. COVID-19. 4. Hibridização *in situ*. 5. Replicação viral. I. Marques-Souza, Henrique, 1977-. II. Universidade Estadual de Campinas. Instituto de Biologia. III. Título.

Informações Complementares

Título em outro idioma: SARS-CoV-2 utilizes incomplete autophagy flux to promote viral replication and cell-to-cell connections to promote cellular evasion
Palavras-chave em inglês:
SARS-CoV-2
Vero cells
COVID-19 (Disease)
In situ hybridization
Virus replication
Área de concentração: Biologia Celular
Titulação: Mestra em Biologia Molecular e Morfofuncional
Banca examinadora:
Henrique Marques Barbosa de Souza [Orientador]
Lucia Elvira Alvares
Fernando Moreira Simabuco
Data de defesa: 29-05-2023
Programa de Pós-Graduação: Biologia Molecular e Morfofuncional

Identificação e informações acadêmicas do(a) aluno(a)
- ORCID do autor: https://orcid.org/0000-0001-8231-1678
- Currículo Lattes do autor: http://lattes.cnpq.br/6347747604580995

Campinas, 29 de Maio de 2023

COMISSÃO EXAMINADORA

Prof. Dr. Henrique Marques Barbosa de Souza

Profa. Dra. Lucia Elvira Alvares

Dr. Fernando Moreira Simabuco

Os membros da Comissão Examinadora acima assinaram a Ata de Defesa, que se encontra no processo de vida acadêmica do aluno.

A Ata da defesa com as respectivas assinaturas dos membros encontra-se no SIGA/Sistema de Fluxo de Dissertação/Tese e na Secretaria do Programa Biologia Molecular e Morfofuncional da Unidade Instituto de Biologia.

I dedicate this work to all my supporters. My family, my beloved husband, my friends and all my pets, who gave me strength to never give up.

ACKNOWLEDGEMENT

My heartfelt thanks go out to Professor Henrique Marques for being an exceptional mentor and friend. You not only provided me with this and many other incredible opportunities, but also believed in me when I didn't believe in myself. I owe a big part of my professional achievements to his unwavering support, trust, and guidance. I am immensely grateful for all the support, encouragement, and teachings you provided during my master's degree and in my life and I will never be able to thank you enough. I would also like to extend my thanks to my laboratory colleagues, in special for Jeruza, Amanda, Giovanna, Paulo, Cyro and Gabriel. You guys made my days and experiments so much funnier and exciting.

My endless gratitude to my parents, Edward and Mirtes, and to my siblings Jack and Gaia. I would not be the scientist I am today without your unwavering support, love, and motivation. I now realize that the occasional scolding was

necessary to keep me on track and focused, and I am grateful for it. This victory is not mine alone, but also yours,

I have not enough words to express all my gratitude, love and admiration to my lab partner, friend and husband, Gabriel. From every experiment to every crisis and victory, you stood by my side, providing invaluable support and motivation. Without your encouragement and push, I would have been stuck in fear and missed out on countless opportunities. I am incredibly fortunate to have shared this cycle with you, and this achievement would not have been possible without your unwavering support. You are incredible, and I am still in disbelief that I was able to capture the heart of someone as pure and wonderful as you. It demands also a second special thanks to UNICAMP, from where I came out with more than a master's degree, but also with a family.

I am immensely grateful to all my "possum friends". You guys made this whole saga much more enjoyable. A special thanks to Aramys, who was there for me through the pandemic and all my existential crises, and was a huge help during the writing of my dissertation. Honestly, I would have probably freaked out if it wasn't for your existence in this pandemic. Shantay, you stay.

Finally, but definitely not less important, I would like to express my endless love to Beto, Iúna, Darwin, Mary, Lolth, Charlotte, Odin, Toco, Sara, Polly, Kiki, Chico and Joana. All I do, I do for you, my babies. The love I feel for you all is the driving force behind my motivation to wake up each day and strive to become the best version of myself.

"Ah, not in knowledge is happiness, but in the acquisition of knowledge! In forever knowing, we are forever blessed; but to know all, were the curse of a fiend."

- Edgar Allan Poe

RESUMO

Em dezembro de 2019, uma nova e altamente contagiosa doença chamada *Coronavirus Disease 2019* (COVID-19), causada pelo vírus de nome síndrome respiratória aguda grave do coronavírus 2 (SARS-CoV-2 – do inglês - *severe acute respiratory syndrome coronavirus 2*) surgiu e rapidamente se espalhou pelo mundo. Tragicamente, a COVID-19 afetou mais de 680 milhões de pessoas, resultando em mais de 6,8 milhões de mortes, especialmente em idosos e aqueles portadores de comorbidades pré-existentes, como hipertensão, diabetes e obesidade. Em resposta a esta pandemia, nosso laboratório e parceiros realizaram pesquisas focadas na detecção de partículas virais de SARS-CoV-2 dentro de células hospedeiras por meio de técnicas de imunofluorescência e hibridação *in situ* (FISH), a fim de analisar sua interação com a maquinaria celular do hospedeiro. Os resultados nas células modelo VERO E6 indicam que, sob infecção por SARS-CoV-2, há uma indução da ativação transcricional da autofagia enquanto genes relacionados a lisossomos e fusão de vesículas são reprimidos. Foi observada o aumento na expressão dos genes relacionados à autofagia AMBRA-1, ATG7, BECN-1 e SNAP29 e queda na expressão do gene VAMP8, responsável por permitir a fusão autofagossomo-lisossomo. Além disso, descobriu-se que partículas virais recém-montadas tendem a se acumular dentro de MVBs/endossomos tardios e autofagossomos, não sendo direcionados para a degradação lisossômica. Os resultados aqui obtidos indicam que o bloqueio do fluxo autofágico completo pode estar envolvido na replicação viral, na proteção contra a detecção imunológica e na disseminação viral através do contato célula-célula. Esta hipótese é apoiada por evidências de inibição da exocitose e colocalização de partículas virais com organelas relacionadas à autofagia. Esses achados podem explicar por que os medicamentos baseados na inibição da autofagia não bloqueiam efetivamente a infecção por SARS-CoV-2. No geral, o estudo fornece informações sobre o mecanismo da infecção por SARS-CoV-2 e destaca a importância potencial da inibição do fluxo de autofagia na promoção da replicação e disseminação viral.

ABSTRACT

In December 2019, a new and highly contagious disease called Coronavirus Disease 2019 (COVID-19), caused by the severe acute respiratory syndrome coronavirus 2 (SARS-CoV-2) emerged and quickly disseminated across the globe. Devastatingly, COVID-19 has affected over 680 people, resulting in more than 6.8 million deaths, especially in elderly individuals and those with pre-existing medical conditions such as hypertension, diabetes, and obesity. In response to this pandemic, our laboratory and partners conducted research focused on the detection of SARS-CoV-2 viral particles inside host cells through immunofluorescence and in situ hybridization (FISH) techniques, in order to analyze their interaction with the host's cellular machinery. The results in VERO E6 cells indicate that, upon SARS-CoV-2 infection, there is an induction of transcriptional activation of autophagy while repressing genes related to lysosomes and vesicle fusion. It was observed up-regulation of autophagy-related genes AMBRA-1, ATG7, BECN-1, and SNAP29 and downregulation of the VAMP8 gene, responsible for allowing autophagosome-lysosome fusion. Additionally, it was found that newly assembled viral particles tend to accumulated within MVBs/late endosomes and autophagosomes, as they could not be targeted for lysosomal degradation. The results here obtained indicate that blockage of complete autophagy flux may be involved in viral replication, protection against immune detection, and viral spread through cell-cell contact. This hypothesis is supported by evidence of inhibition of exocytosis and colocalization of viral particles with autophagy-related organelles. These findings may explain why drugs based on the inhibition of autophagy do not effectively block SARS-CoV-2 infection. Overall, the study provides insights into the mechanism of SARS-CoV-2 infection and highlights the potential importance of autophagy flux inhibition in promoting viral replication and spread.

FIGURE LIST

LIST OF ABBREVIATIONS

ACE2 - angiotensin-converting enzyme 2

AMPK - AMP-activated protein kinase

ATG - Autophagy-Related Genes

BSA - Bovine Serum Albumin

CMC - Carboxymethyl cellulose

CN - Negative control

CoVs – Coronaviruses

DEPC - Diethyl dicarbonate

DMEM - Dulbecco's modified Eagle medium

DMV - Double membrane vesicles

DUTP - Deoxyuridine

E – Envelope

EBOV - Ebola

ERGIC - Endoplasmic-reticulum–Golgi intermediate compartment

FBS - Fetal Bovine Serum

FISH - Fluorescent in situ hybridization

HCV - Hepatitis C Virus

HIV - Human immunodeficiency virus

HPI – Hours post infection

HSV - Herpes simplex virus

HYB - Hybridization

IF - Immunofluorescence

LC3 - Microtubule-associated Protein 1 Light Chain 3

M - Membrane

MERS - Middle East Respiratory Syndrome

MOI - Multiplicity of infection

MTOR - mammalian target of rapamycin

MVBs - Multivesicular bodies

N - Nucleocapsid

NSP - Non-structural proteins

PC – Positive Control

PBS - Phosphate-Buffered Saline

PCR - Polymerase chain reaction

PFA – Paraformaldehyde

PFU - Plaque-Forming Units

RdRp - RNA-dependent RNA polymerase

RSV - Respiratory Syncytial Virus

RT-qPCR - Reverse transcription-quantitative polymerase chain reaction

RT-PCR - Real Time-Polymerase Chain Reaction

S - Spike

SARS - Severe Acute Respiratory Syndrome

SARS-CoV-2 - Severe Acute Respiratory Syndrome 2

SNAP29 - Synaptosome associated protein 29

SNARE - Soluble NSF Attachment Receptor

SSC - Saline-Sodium Citrate buffer

STX17 - Syntaxin 17

TMPRSS2 - M protease serine 2

ULK - Unc-51-like Kinase

VAMP7/VAMP8 - Vesicle Associated Membrane Protein 7/8

β-coronavirus – Betacoronavirus

SUMARY

INTRODUCTION

Impact of viruses in human health

Viruses are a diverse group of significant pathogens that play crucial roles in the environment, having evolved to infect a wide range of hosts in order to replicate (*1, 2*). Certain viruses are specifically responsible for causing serious illnesses in humans and animals (*3*), resulting in constant impacts on global public health due to emerging viral infections (*4*), with acute respiratory infections being among the most common ailments affecting humans (*5, 6*).

Respiratory infections, particularly those affecting very young or elderly individuals with seasonal occurrences, are a significant driver of high healthcare costs (*5, 7*). Influenza, respiratory syncytial virus (RSV), and rhinovirus are the main culprits behind these infections. However, since 2002, coronaviruses have become a growing concern (*4*), given the rising global numbers of infections and deaths, as well as the lack of specific medical treatments or drugs to effectively contain the threats posed by these coronaviruses, which also have economic implications worldwide (*8*).

Coronaviruses (CoVs) are positive single-stranded RNA viruses that belong to the Coronaviridae family (*9*). The family has four genera, with Gammacoronavirus and Deltacoronavirus mainly infecting birds, while Alphacoronavirus and Betacoronavirus (β-coronavirus) are associated with respiratory infections in a variety of mammals (*10, 11*). In humans, seven species of CoVs are known to cause infection (*12*). Among them, β-coronaviruses are of particular concern due to their ability to cross the animal-human barriers and cause human disease (*8, 13*), as seen in the virulent epidemics of Severe Acute Respiratory Syndrome (SARS) and Middle East Respiratory Syndrome (MERS) (*14*). Recently, a pandemic was triggered by a novel β–coronavirus, known as severe acute respiratory syndrome coronavirus 2 (SARS-CoV-2), causing a new infectious disease known as COVID-19 (*15*).

Severe Acute Respiratory Syndrome *and COVID-19*

First detected in Wuhan, China, in December 2019, SARS-CoV-2 has quickly spread across the globe, infecting over 680 million people and causing more

than 6.800.000 deaths in more than 220 countries (*16*). Its ability to rapidly propagate (*12*), as well as its high contagion and mortality rates in certain risk groups (*17–20*), prompted the World Health Organization to declare a pandemic on March 11, 2020 (*21*).

SARS-Cov-2 is a spherical-shaped virus, covered with a large number of glycosylated spike protein (S), giving it the appearance of a crown (*8*). In addition to the Spike protein, the virus also has three other structural proteins: nucleocapsid (N), which forms the capsid outside the genome, and the proteins M (membrane) and envelope (E), which together with Spike are associated to the envelope that that encloses the viral genome (*22*, *23*). Sixteen non-structural proteins (nsp1−16) are involved in basic viral processes such as replication, modulation of host cells' survival signaling, methylation of viral mRNAs and protein synthesis (*22*). Additionally, the Spike protein not only plays a structural role but also functions as the key mediator for viral entry into host cells. This process involves the binding of the viral Spike protein to the host cell receptor ACE2 (angiotensin-converting enzyme 2), as well as its activation by $TMPRSS2$ (M protease serine 2) enzyme on the host cell membrane, which triggers viral entry (*8*, *23*).

Several studies have demonstrated a remarkable genomic structural resemblance between SARS-CoV-2, SARS-CoV, and to a lesser extent, MERS, the most pathogenic viruses of the β-coronavirus genus (*11*, *24*). Phylogenetic tree analysis has further revealed that SARS-CoV-2 and SARS-CoV belong to the same clade and share the same human cell receptor, which is distinct from MERS (*25*).

Despite sharing similarities, SARS-CoV-2 has been shown to have lower pathogenicity and fatality rates in comparison to SARS-CoV and MERS. However, COVID-19 has caused significantly more deaths worldwide (~6.897.000) (*26*, *27*) than both SARS and MERS combined (~1802) (*28–30*), likely due to its faster human-to-human transmission rate (*29*). The highly transmissible nature of COVID-19 can be attributed to its less severe clinical symptoms and its distinct tropism for the upper respiratory tract (*25*). Additionally, the viral load reaches its highest point before the onset of symptoms and is higher in the nose than the throat (*31*, *32*). The viral load decreases within days, indicating a higher spread capacity of SARS-CoV-2

in comparison to SARS-CoV, whose highest elimination rate occurs after 10 days from symptom onset (*25*).

While the symptoms of COVID-19 are generally milder than those of SARS and MERS, they are still not fully determined (*29*), but includes fever, headache, cough, sore throat, fatigue, myalgia and shortness of breath, which can progress to pneumonia, respiratory failure and death (*33*). People of all ages are susceptible to the virus, but the likelihood of infection increases with age (*34*), particularly for elderly individuals and those with pre-existing medical conditions such as hypertension, diabetes, obesity, and heart disease, who are more prone to experiencing severe symptoms (*35, 36*).

As the impact of covid-19 continues to spread, it is crucial to understand how the virus interacts with the host's immune system.

Autophagy pathway and its role in viral infections

Autophagy is a catabolic and genetically regulated cellular process that plays a crucial role in maintaining cellular homeostasis and promoting cellular renewal through lysosomal-mediated degradation of cytoplasmatic material, including damaged proteins and organelles (*37, 38*).

In general, autophagy is typically induced when nutrients are limited, in order to produce amino acids that can be converted into glucose to meet the body's energy requirements (*39*). The process is regulated by nutrient conditions, particularly through the action of mTOR (mammalian target of rapamycin) (*40*). During periods of starvation, autophagy culminates in the degradation of engulfed cellular components by degradative lysosomal enzymes through the fusion of autophagosome-lysosome, which is mediated by SNARE (soluble NSF attachment receptor) complexes, including STX17-SNAP29-VAMP7/VAMP8 (*41*).

In addition to removing unnecessary or dysfunctional cellular components, autophagy plays a crucial role as a frontline defense against intracellular pathogens. such as viruses (*42*) (virophagy), through a process of macroautophagy known as xenophagy (*43*). However, certain viruses have developed mechanisms to evade autophagy (*44*), avoid the immune response (*45*) and hijack autophagosomes for viral replication (*46*), as observed in respiratory syncytial virus (RSV) and the

hepatitis C virus (HCV) (*47, 48*). While it is known that most CoVs can interact with the autophagy machinery to promote viral replication, the exact relationship between CoV infection and autophagy remains unclear (*49*).

The modulation of autophagy can benefit viral infections in several ways, such as serve as delivery vehicle for viral particles (*50, 51*) and act as a replication platform, as the autophagosome can concentrate nutrients, offer structure and promote protection against immune detection (*52–56*); Additionally, the autophagy process can provide nutrients necessary for viral replication (*57*), facilitate the late stages of the viral lifecycle, such as maturation and egress (*58, 59*), and prevent the virus from undergoing degradation and host's programmed cell death (*50, 60–62*).

As virophagy can be either proviral or antiviral (*63*), depending on target's ability to hijack it, there is different ways in which autophagy acts on the host or is modulated by viruses. In a host-positive scenario, autophagy selectively targets viruses to be engulfed by autophagosomes and degraded by lysosomal activity, leading to integration with innate pattern recognition receptor signaling, which induces host's interferon (IFN)-mediated viral clearance, and activating host innate immune response (*64*). However, in a proviral scenario, viruses are capable to subvert host autophagy by inhibiting autophagy activation through blockage of host ATG protein function, modulation of host autophagy for self-benefit in viral replication and inhibition of autophagy downstream degradation pathway (*65*).

In addition to modulating autophagy, viruses can exploit other cellular mechanisms to enhance their success, such as cell-cell contact, which will be discussed below.

The role of cell-to-cell contact in viral spread

The success of viruses depends on their ability to evolve and replicate efficiently (*66*). For this purpose, in addition to replication, viruses must evade the host's immune system and spread effectively.

One way in which viruses achieve successful pathogenesis is through the manipulation of cell-cell contact, which allows for their spread while evading neutralizing antibodies, contributing to immune evasion (*67*). This mechanism is

exploited by numerous medically important viruses, particularly those that are highly pathogenic, such as HIV (*68, 69*), HCV (*70, 71*), HSV-1 (*72*) and EBOV (*73*).

In general, cell-cell spread occurs through the hijacking of cytoskeletal networks, coordinating a complex interplay between actin and microtubube (*74*). This results in the formation of filopodia, nanotubes, actin tails, and, following cell-to-cell fusion, a giant single cell with numerous nuclei, called a syncytium (*75*).

Insights in SARS-CoV-2 infection

Unlike MERS and SARS, SARS-CoV-2 viral load reaches its peak before symptoms appear and is capable to maintain high levels of viral shedding for as long as three weeks (*31, 76*), allowing for its silent spread. However, it is still unclear how SARS-CoV-2 is capable to proliferating and evading detection by the immune system in the early stages of the disease. As here discussed, a wide variety of viruses can evade the immune system through cell-to-cell transmission, while replication is facilitated by the hijacking of autophagy flux. The occurrence of one or both of these mechanisms could explain the high success of SARS-CoV-2 in becoming a pandemic.

Inspired by the topics here discussed, the aim of this work is to detect SARS-CoV-2 particles in infected cells and study the viral dynamics within cells using double immunofluorescence and confocal imaging.

OBJECTIVES

General: To detect SARS-CoV-2 viral particles inside host cells and examine their interactions with the host's cellular machinery.

Specifics:

1. To detect SARS-CoV-2 cellular receptor ACE-2 in both mock and infected VERO E6 and cells.

2. To detect SARS-CoV-2 particles in VERO E6 cells during the first 24h of infection.

3. Codetection of SARS-CoV-2 particles and its cellular receptor ACE-2 in infected VERO E6 cells.

4. To detect the SARS-CoV-2 genome inside cells via fluorescent in situ hybridization.

5. Codetection of SARS-CoV-2 particles and markers of cellular components and Autophagy-related factors via immunofluorescence.

6. To detect SARS-CoV-2 particles in cell-to-cell connections by in situ hybridization.

7. Codetection of SARS-CoV-2 particles and the late endosome marker CD63 in cell-to-cell connections via immunofluorescence.

MATERIAL AND METHODS

Cellular culture, infection and related analysis

- **Cell culture and viral infection**

Cultures of cellular models VERO E6 (African green monkey kidney cells - *Cercopithicus aethiops*) and A549 (adenocarcinomic human alveolar basal epithelial) were maintained at 37 °C and 5% CO_2 in DMEM (Sigma-Aldrich, USA) with 10% heat-inactivated FBS (Sigma-Aldrich, USA) and 1% of antibiotics Penicillin (100 U/mL; Sigma-Aldrich, USA) and Streptomycin (100 µg/mL; Sigma-Aldrich, USA). The Brazilian isolate SARS-CoV-2/SP02/human/2020/BRA (GenBank: MT126808) was generously provided by Professor Edison Luiz Durigon (University of São Paulo) for infection assays. For all experiments described here, virus propagation was carried out in VERO E6 cells (*77*) in the Biosafety Level 3 Laboratory (BSL-3) of the Laboratory of Emerging Viruses for all experiments here described. For viral infections, VERO cells were seeded in 24-well plates (5×10^5 cells/well) using the multiplicity of infection (MOI) of 1.

- **Plaque-forming units' assay (PFU)**

The PFU assay was used to determine the viral titer in both experimental samples and infected cell supernatant, which was performed as previously described (*77*), with slight alterations. Briefly, six 10-fold dilutions of the prepared samples were added (duplicate) to VERO E6 cells seeded in 24-well plates (5×10^5 cells/well), along with SARS-CoV-2 positive and negative controls, and incubated for 1 hour on a rocking platform (room temperature). After viral adsorption, 1% CMC semisolid medium (Sigma-Aldrich, USA), prepared with DMEM supplemented with 2% FBS and 1% of penicillin-streptomycin, was added to the wells and incubated at 37°C and 5% CO_2 for 48 hours. Following incubation period, the semisolid medium was removed, and the cells were subsequently fixed with 8% paraformaldehyde, followed by a wash with distilled water, before being stained with methylene blue (Sigma-Aldrich, USA).

To assess the quantity of viable viral particles produced within VERO E6 cells, the first step was to remove the supernatants from the wells. Then, the cells were washed with 1x PBS before collecting the monolayer, which was rapidly frozen

using liquid nitrogen. Subsequently, the frozen cells were subjected to three rounds of freeze-and-thaw cycles in liquid nitrogen and a 37 °C water bath. Finally, the resulting samples were titrated by PFU to determine the viral titer.

- **Bafilomycin treatment**

Vero E6 cells cultured in 24-well plates (5×10^5 cells/well) were removed from incubation and washed once with PBS, followed by treatment for 3 hours with 10 mM of bafilomycin prepared in DMEM supplemented with 10% FBS. The treatment was ceased 2 hours before infection, and at 24 hpi, plaque-forming units (PFU) were used to determine the titers of the cells and supernatant samples, using previously described methods.

In situ hybridization and immunofluorescence

- **Probe synthesis**

To generate the probe for SARS-CoV-2 RdRp mRNA, two sets of Polymerase Chain Reaction (PCR 1 and PCR 2) were performed. In PCR1, SARS-CoV-2 target gene was amplified using GoTaq® DNA Polymerase kit (Promega - M3008) and specific oligonucleotide primers for viral RdRp (Forward 5'-AACACGCAAATTAATGCCTGTCTG 3', Reverse 5' GTAACAGCATCAGGTGAAGAAACA 3') and the reactions were performed using GoTaq® DNA Polymerase kit (Promega - M3008). Each reaction was set up with 0.25 µL of GoTaq® DNA Polymerase (5 u/µL), 1 µL of each SARS-CoV-2 RdRp primer (10 mM), 1 µL of viral cDNA (1:10 dilution) (prepared using High-Capacity cDNA Reverse Transcription Kit by Thermo Scientific - 4368814, following the manufacturer's instructions), 1 µL of dNTP mix (10 mM), 2 µL of $MgCl_2$, 10 µL of 5X GoTaq reaction buffer, and 33.75 µL of nuclease-free water to a total volume of 50 µL. The reactions were then subjected to a thermocycler (Eppendorf® Mastercycler® EP) program with the following steps: Initial denaturation - 95 °C for 2 min; 35 cycles of Denaturation - 95 °C for 30s; Annealing - 55 °C for 30 s; Elongation - 72 °C for 30s; and final extension - 72 °C for 5 min.

Next, PCR 2 was performed in order to incorporate biotin molecules into the probe. For this purpose, the appropriate unlabeled dNTP was replaced with bio-16-dUTP (Sigma-Aldrich – 11388908910) to be added to the reaction mix. Each reaction of PCR 2 was prepared using almost same proportions described

previously. However, in place of cDNA, 1 µL of PCR 1 product as used as DNA template while 1 µL of d (A, C, G) TP (10 mM), and 0.5 µL of 16dUTP (0.2 mM) was applied instead of dNTP mix. PCR 1 and PCR 2 programs were the same. At the end of PCR 2, the newly synthesized complementary DNA strands incorporate the biotin-16-dUTP, resulting in a 300 bp biotinylated DNA probe with the following sequence:

5'-
AACACGCAAATTAATGCCTGTCTGTGTGGAAACTAAAGCCATAGTTTCAACTATA
CAGCGTAAATATAAGGGTATTAAAATACAAGAGGGTGTGGTTGATTATGGTGCT
AGATTTTACTTTTACACCAGTAAAACAACTGTAGCGTCACTTATCAACACACTTAA
CGATCTAAATGAAACTCTTGTTACAATGCCACTTGGCTATGTAACACATGGCTTA
AATTTGGAAGAAGCTGCTCGGTATATGAGATCTCTCAAAGTGCCAGCTACAGTT
TCTGTTTCTTCACCTGATGCTGTTAC-3'.

Fluorescent In situ Hybridization (FISH)

VERO E6 infected and mock cells were removed from culture medium and submitted for 20 minutes to fixation on 4% PFA (pH 7.40), prepared in PBS-DEPC (pH 7.4). Next, cells were submitted to PBS-DEPC washing process for three times prior exposition for 30 minutes, at room temperature, to a 2% H_2O_2 solution prepared in methanol. This step was performed protected from the light, in order to avoid autofluorescence. After incubation time, cells were submitted again to washing step and incubation in Proteinase K (10 µg/mL) solution prepared in PBS-DEPC-Tween 0.1 M (pH 7.4) for 2 minutes, enabling its permeabilization. Subsequently, a glycine solution (2 mg/mL) diluted in 0.1M PBS-DEPC-Tween (pH 7.4) was applied for 10 minutes at room temperature to inactivate the previously step. Finally, a second fixation and washing step was performed, but for only 10 minutes.

The following step was to perform the Hyb itself. First, the Hyb solution composed of 50% formamide, 10% dextran sulfate and 2x SSC (pH 7) was prepared and supplemented with salmon sperm DNA (2 µg/mL) for 2 hours at 37 °C using a humid box, in order to avoid nonspecific signals. Next, the cells were incubated in Hyb solution with the biotinylated probe (100 µL/mL) prepared previously, which was denatured at 85 °C and then added to the cells. After incubating the cells in a humid box at 37°C for 16 hours, the hybridization solution was gradually removed by washing the cells with a 50% Hyb + 2x SSC (pH 7) solution for 20 minutes at 37°C,

followed by washing with a 25% Hyb + 2x SSC (pH 7) solution, a washing using a 2x SSC solution for 10 minutes at 37 °C and a final washing using PBS-DECP 1X at least 5 times, in order to remove any remaining Hyb or SSC residues, as well as excessive probe that was not hybridized. In the final step, the samples were incubated protected from the light at room temperature for 2 hours with Streptavidin (Invitrogen #21842) diluted (1:500) in PBS-DEPC 1X, and then washed using PBS to remove any excess of Streptavidin. Finally, cells were incubated with DAPI (Santa Cruz Biotechnology - #SC-3598) for 10 minutes at room temperature while being protected from light, using a dilution ratio of 1:1000 in PBS (Ph 7.4).

Samples were imaged using a confocal microscopy (Zeiss – Airyscan/LSM880) on an inverted microscope (Zeiss - Axio Observer 7/ 491914-0010-000) with a C Plan Apochromat 63x/1.4 Oil DIC objective, 4x optical zoom. Before conducting image analysis, the raw.czi files underwent automatic processing through the Zen Black 2.3 software to produce deconvoluted Airyscan images. The DAPI images were obtained by means of conventional confocal imaging, utilizing a 405 nm laser for excitation and setting the pinhole aperture to 1 AU.

- **Immunofluorescence**

For immunofluorescence, Vero E6 and A549 cells were removed from culture medium and fixed in salinized glass slides using 4% PFA, following by a wash step using PBS-Tween (pH 7.4) and incubation with 0.1 M glycine for 10 minutes. Next, the cells were treated with a BSA solution (Sigma - A8327) for 30 minutes prior antibodies application. Primary antibodies were diluted in PBS-Tween and 1% BSA (1:100), added to the fixed cells using the desired double IF combination* and incubated overnight at 4 °C. Next day, washing step was repeated and the slides were incubated for 2 hours with secondary antibodies** diluted (1:500) in PBS-Tween + 1% BSA, followed by new washing process. Then, a final staining process using DAPI (Santa Cruz Biotechnology, #SC3598) was performed, in order to stain the nuclei, and the samples were imaged as previously described.

* SARS-COV-2 Spike S1 antibody (#HC2001 GenScript - #A02038); Lamp1 antibody (#BD 555798); p62 antibody (#BD 610832); and CD63 antibody (#BD 556019)]

** (Alexa 488 anti-Human IgG Thermo Fisher #A11013; Alexa Fluor 555 Anti-Mouse IgG #A21422).

Molecular analysis

- **RNA extraction and cDNA synthesis**

Cell types submitted to infection and molecular analysis were kept in culture until reaching confluence. Subsequently, the cells were collected and centrifuged at 13,000 RPM for 5 minutes to obtain a pellet, which was transferred to Eppendorf tubes and added with 1 mL of TRIzol (Thermo Fisher – 15596018) while being kept refrigerated. After adding TRIzol, the solution was incubated for 7 minutes, followed by the addition of 200 µL of chloroform (Sigma-Aldrich - P4557) per tube, manually shaken for 15 seconds and incubated for 3 minutes. The samples were then centrifuged at 12,000 RPM for 15 minutes at 4°C, leading to the separation of the solution into 3 phases. The first phase was transferred to a new Eppendorf tube using a pipette, and 500 µL of isopropyl alcohol (Sigma-Aldrich - G2526) was added, following by manually shaken and inversion. After incubating for 10 minutes at room temperature, the samples were centrifuged at 12,000 RPM for 15 minutes at 4°C, and the resulting supernatant was discarded. The pellets were washed with 75% ethyl alcohol and centrifuged at 12,000 RPM for 5 minutes at 4°C. The supernatant was discarded, and the pellets were left to dry completely at room temperature for around 20 minutes. The pellets were dissolved in DEPC-water and quantified using a NanoDrop® 2000 spectrophotometer (Thermo Scientific). The integrity of the samples was assessed using 1% agarose gel electrophoresis and visualized under UV light. After RNA extraction, cDNA was synthesized using the High-Capacity cDNA Reverse Transcription Kit (Thermo Scientific - 4368814), following the manufacturer's instructions.

- **Gene selection and primers design**

Key genes related to the different phases of the autophagic pathway were selected, as well as genes likely to play a role in the viability of cellular-to-cellular viral transfer. The primers used were taken from the Harvard University (Primer Bank - https://pga.mgh.harvard.edu/cgi-bin/primerbank/new_search2.cgi) and had them synthesized by Exxtend - Soluções em Oligos. To ensure the quality of the primers,

we amplified the chosen genes using conventional PCR with the GoTaq® DNA Polymerase PCR kit (Promega - M3008), following the manufacturer's recommendations, for a final volume of 10µL. We analyzed the resulting PCR products by 1% agarose gel electrophoresis, considering the expected amplicon size during primer design and the obtained band size, using the GeneRuler 1 kb DNA ladder (Thermo Scientific - SM0311), as parameter.

- **Analysis of gene expression by RT-qPCR**

The cDNAs obtained from control and infected cells were utilized to perform RT-qPCR analysis of target gene expression. For each gene and cell type, 8 µL of SYBR® Green (Biorad - 4364344) supplemented with the recommended dye, 4.5µL of cDNA (1:10 dilution), and 4.5 µL of primer (10 µM) were added to a 0.6 ml Eppendorf tube. After homogenization, 5 µL of the solution was applied per well of the qPCR plate (Kasvi 384 wells) in triplicate, using GAPDH as an endogenous control. For the VAMP8 gene, a 50x cycle was used due to its low expression. The plate was then sealed with a sealing film (Kasvi), centrifuged at 2,000 RPM for 30 seconds, and inserted into the CFX384 Touch System (Bio-Rad) for a 40x cycle, as per the manufacturer's recommendation. Upon completion of the program, the data obtained was analyzed using Bio-Rad CFX Manager and Excel software to calculate the CT deltas and gene expression. The resulting graphs were prepared using GraphPad Prism 5.0 software, comparing the gene expression in infected cells vs mock and VERO E6 vs A549, due to the high and low infection rates of the respective cell types.

Statistical analysis

Statistical analysis of PFU and RT-qPCR was performed using GraphPad Prism 9.0 and 8.0, respectively. The presented values represent the mean and standard deviation (SD), and the mean difference was tested using a T-test. Significance was set at $p < 0.05$.

RESULTS AND DISCUSSION

Due to the COVID-19 pandemic caused by SARS-CoV-2, all experiments unrelated to this virus was interrupted at the university and the laboratories redirected they attention to study the virus. In April 2020, our laboratory - Brazilian Laboratory on Silencing Technologies - initiated a study on SARS-CoV-2 by detecting ACE2 expression 24 hours post-infection (hpi) using antibodies in VERO E6 cells (**Figure 1**) and A549 cells (**Figure 2**), which are two initial model cells commonly used for SARS-CoV-2 studies (*78, 79*).

The immunofluorescence analysis revealed a significant abundance of ACE2 receptors in VERO cells (**Figure 1 B**, **C**), while A549 showed negligible levels (**Figure 2 B**, **C**), which was consistent with later published studies demonstrating that A549 cells are poorly infected with SARS-CoV-2 due to low ACE2 receptor expression on the cell membrane (*80, 81*). The abundance of ACE2 in both mock and infected VERO E6 cells, when compared to A549, was also consistent with literature (*82, 83*). Interestingly, the immunofluorescence of infected cells showed a lower rate of ACE2 receptor presence when compared to mock (**Figure 1 C**). This result is compatible with a study performed with SARS-CoV, in which a downregulation of ACE2 protein levels was observed after infection, inversely correlated with viral replication, indicating a strong receptor interference after viral Spike bound to ACE2 in VERO cells and post-transcriptional regulation of ACE2 proteins (*84, 85*).

Due to their high expression of ACE2 receptor and consequently greater susceptibility to SARS-CoV-2 infection, VERO E6 cells were selected as the primary model to be used for subsequent experiments here described.
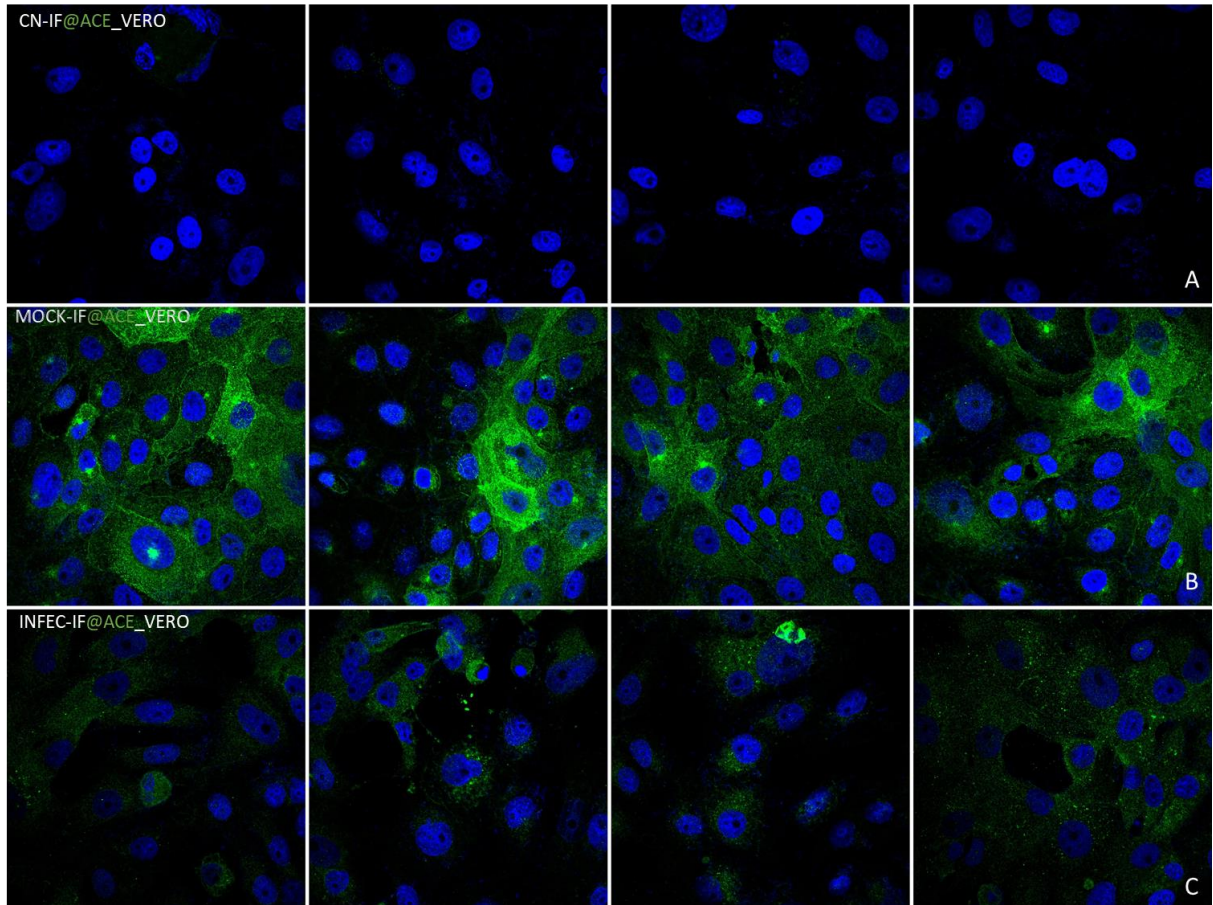
Figure 1.**Immunofluorescence analysis for the detection of ACE2 receptor in VERO E6 cells.** Immunofluorescence staining for the detection of cellular receptor ACE2 in VERO cells 24 hpi revealed a high abundance of these receptor in mock cells **(B),** and a lower rate, but still significant, in infected cells **(C).**
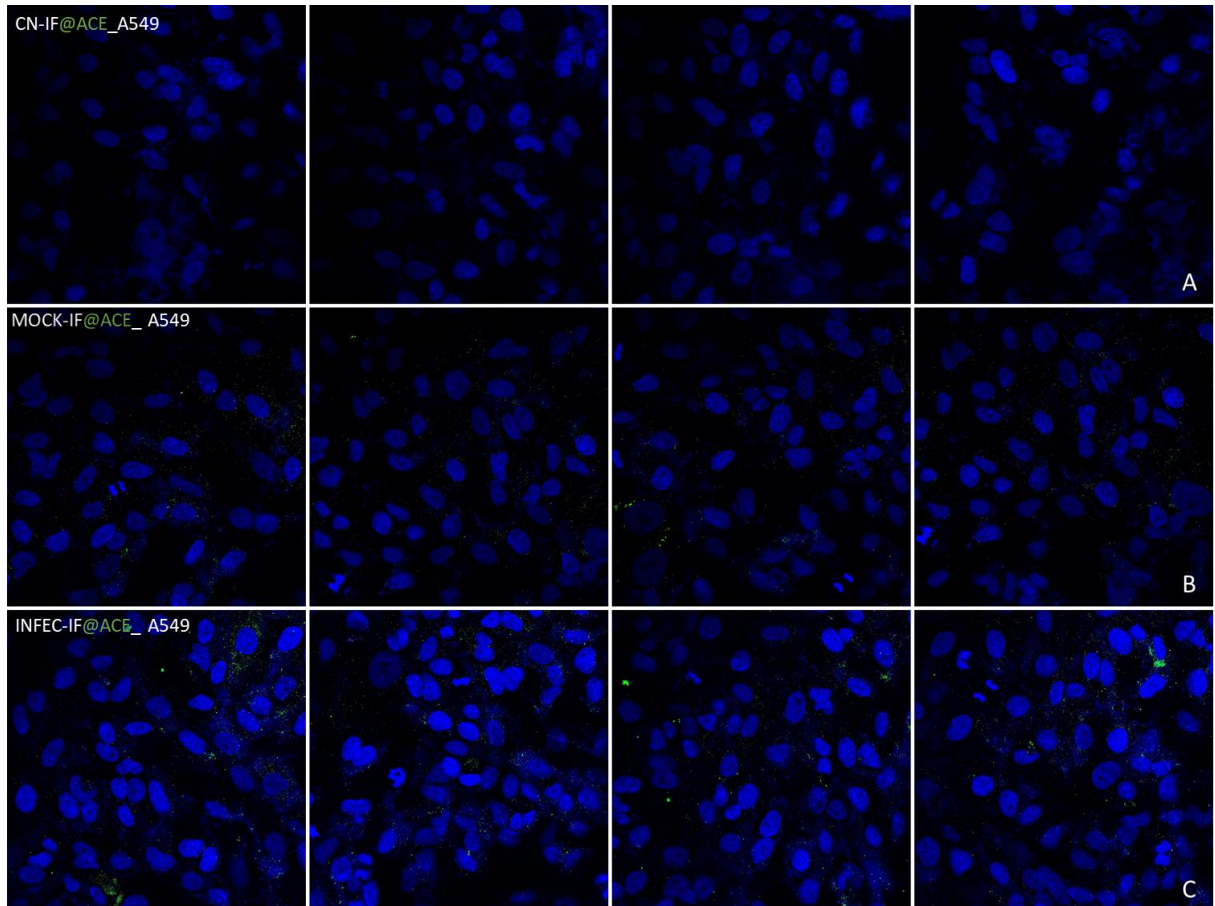
Figure 2. **Immunofluorescence analysis for the detection of ACE2 receptor in A549 cells.** Immunofluorescence staining for the detection of cellular receptor ACE2 in A549 cells 24 hpi, revealed a poor presence of these receptor in both mock and infected cells **(B, C).**

After characterizing the ACE2 pattern in our chosen model cell, an immunofluorescence analysis was conducted to detect viral particles in VERO E6 cells using antibodies for viral protein Spike and cellular ACE2 (**Figure 3**). A high level of infection was observed in VERO cells 24 hpi, as expected based on the literature (*82*) (**Figure 3 C-D'''**). Interestingly, viral labeling was identified as circular structures (**Figure 3 C''**, **D''**), very similar to multivesicular bodies (MVBs) (**Figure 3 C'**, **D'**).
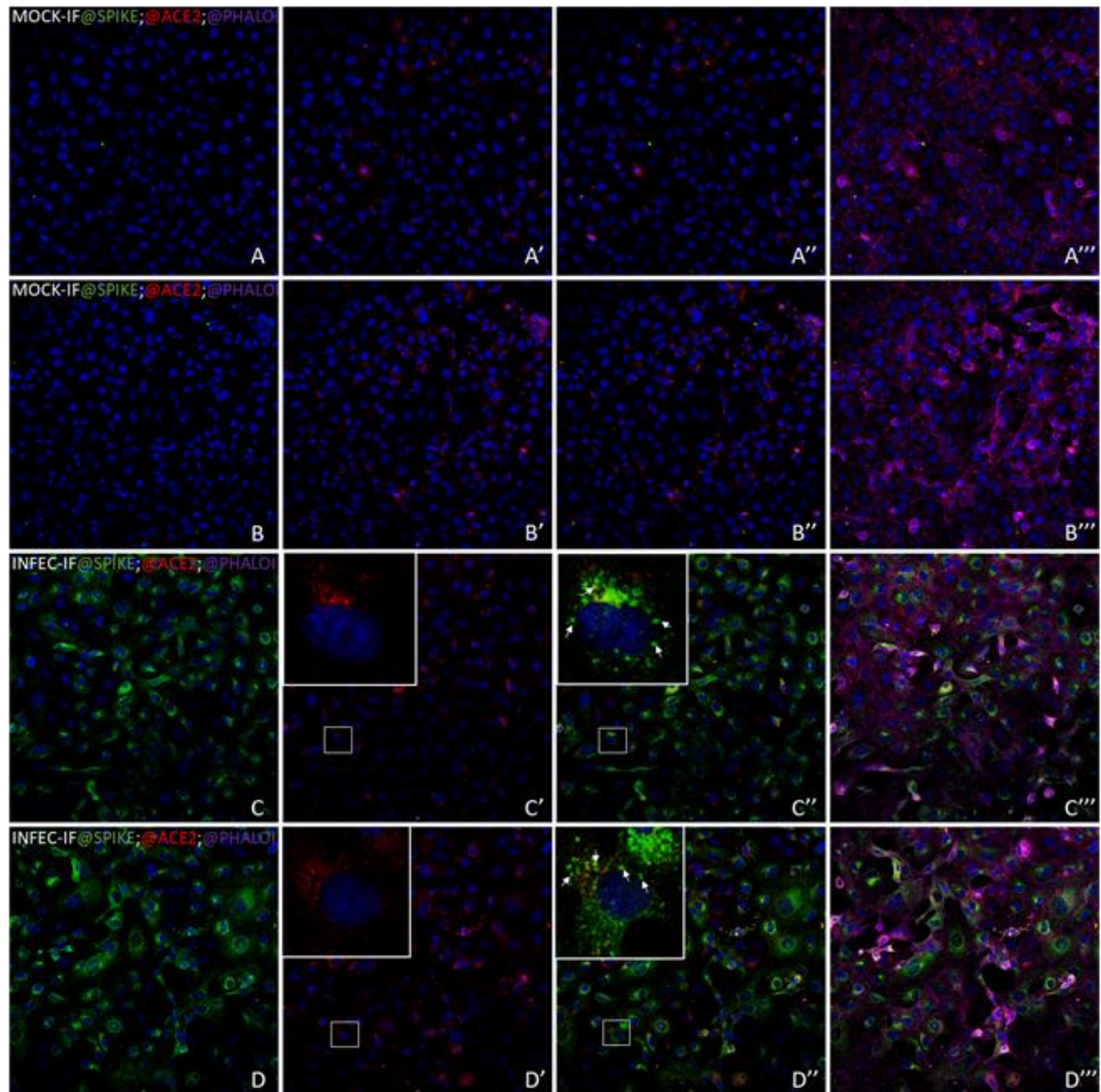
Figure 3. Immunofluorescence analysis for the detection of viral Spike protein and ACE2 receptor in VERO E6 cells. Immunofluorescence staining for the detection of viral Spike protein (green) and cellular receptor ACE2 (red) in VERO mock **(A, B)** and infected **(C, D)** cells 24 hpi, demonstrating a high presence of viral particles in infected cells and circular structures containing Spike protein near the cellular nucleus (highlighted in C'', D'')**.**

During the early experiments of COVID-19 disease, our laboratory developed a low-cost fluorescent in situ hybridization (FISH) method using biotinylated DNA probe targeting SARS-CoV-2 RNA dependent RNA polymerase (RdRp) mRNA to specifically detect and visualize SARS-CoV-2 in VERO cells (*86*). This allowed us to visualize the viral genomic RNA and identify MVB-like structures

(**Figure 4**), similar to those revealed by immunofluorescence for Spike protein (**Figure 3**).

While no MVB-like FISH labelling was observed in the negative control (**Figure 4 A**) or mock (**Figure 4 B**), highlighting the probe's specificity, MVB-like FISH labeling confirmed the presence of viral particles in infected cells (**Figure 4 C**, **D**). Interestingly, MVB-like labeling was predominantly observed around the cellular nucleus (**Figure 4 C-D''**), with some MVB-like labeling observed also in the cytoplasm and in cytoplasmatic projections (**Figure 4 D'**, **D''**).

To better understand the dynamics of SARS-CoV-2 infection, Spike protein IF was performed in VERO E6 infected (MOI 1) cells after 12, 16, 20 and 24 hpi, counter-labeling these cells with F-actin/cytoskeleton marker Phalloidin (**Figure 5**). The time point selection was based on viral replication rate, which starts approximately 7-8 hpi, increasing exponentially until 12 hpi, corresponding to the time of appearance of infection foci (*87*, *88*).
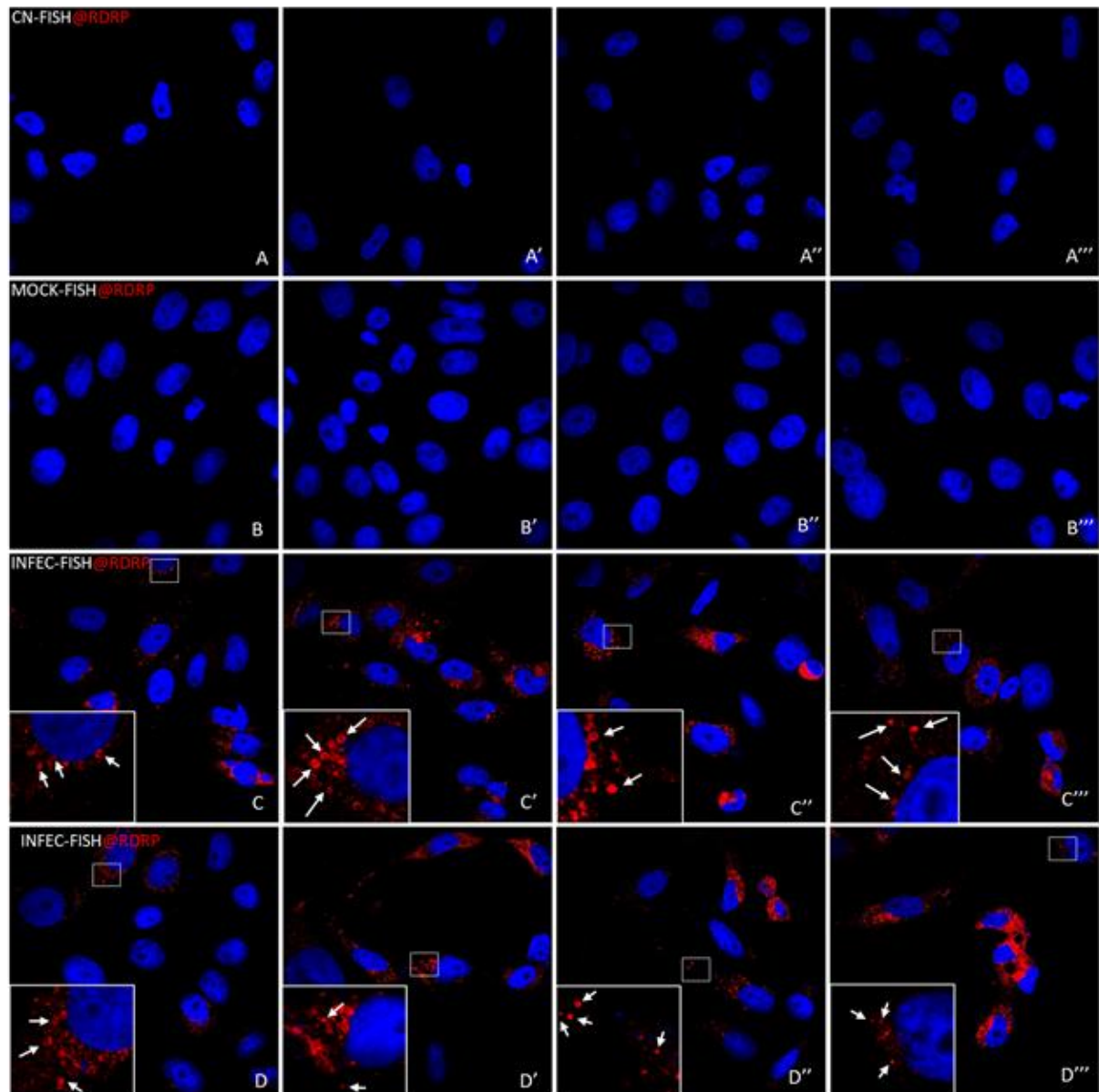
Figure 4. Fluorescent *in situ* hybridization to detection of viral mRNA of RdRp (C, D) in VERO E6 cells. Fluorescent *in situ* hybridization for detection of viral RdRp (red) in VERO E6 cells 24 hpi, evidencing the presence of SARS-CoV-2 particles in MVB-like structures **(C, D)**, with no similar structures observed in CN **(A)** or mock **(B).**

Spike IF detected the presence of viral particles inside VERO cells at 12 hpi (**Figure 5 A-A'''**), with a strong increase in labeling intensity and number of labeled cells at 16 hpi (**Figure 5 B-B'''**), which persisted until 24 hpi (**Figure 5 B-D'''**). Cell cytoplasm and membrane retraction were also observed, starting at 16 hpi (**Figure 5 B**) and progressively increasing in robustness at 20-24 hpi (**Figure 5 C-D**). However, no further investigation was conducted to confirm the nature of this alteration. Similar to previous reports for VERO E6 cells infected with SARS-CoV-2 (*89*), we observed signs of cell rounding, detachment, degeneration, and syncytium formation (**Figure 5 C-D**). Interestingly, Chu and collaborators (2020) reported that despite the robust damage caused by SARS-CoV-2 in VERO E6 cells, this damage is lower compared to those caused by SARS-CoV, as the cell viability was significantly higher after SARS-CoV-2 infection than those by SARS-CoV at multiple times and same MOI, supporting its lower fatality rate and milder symptoms.
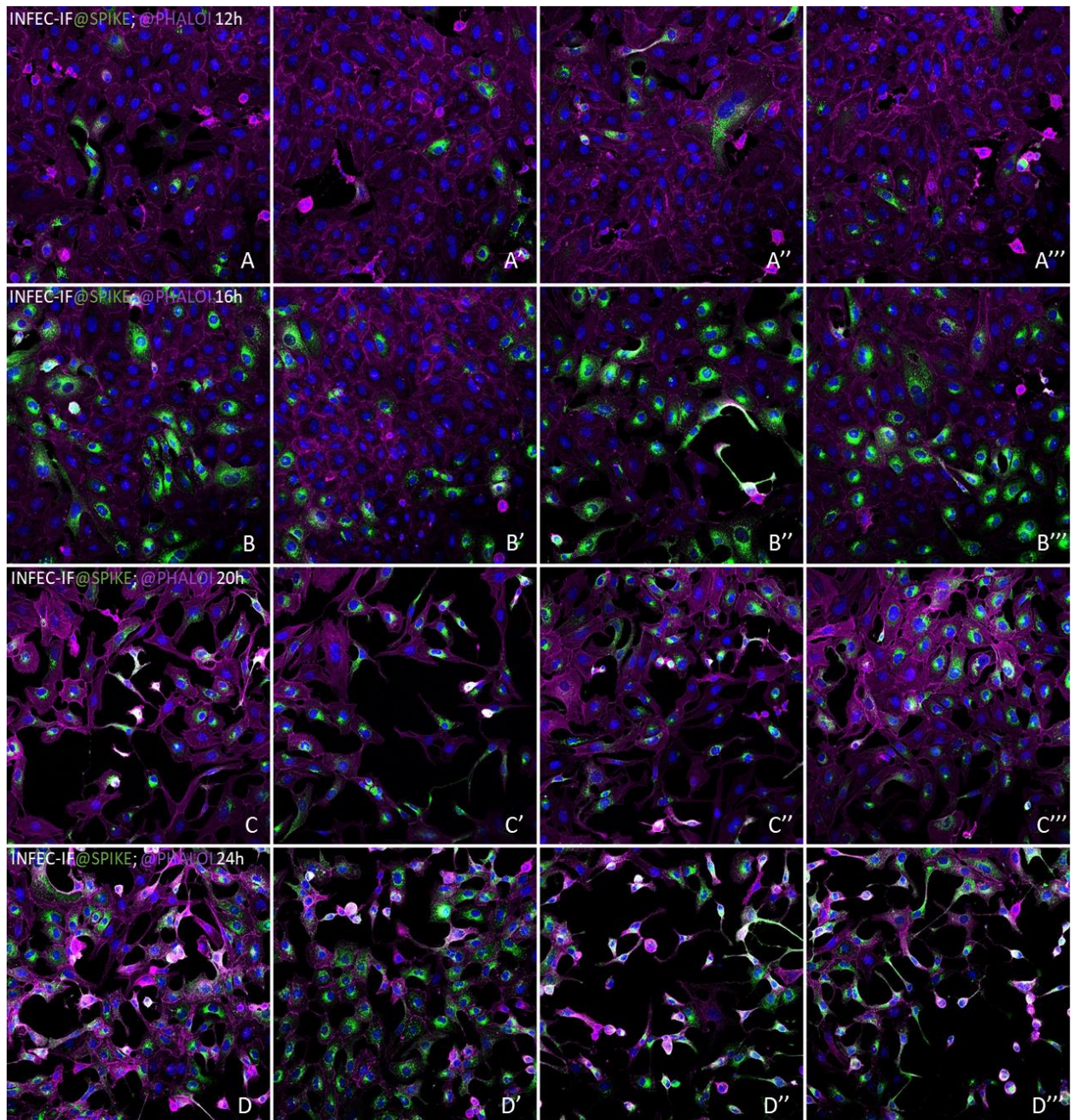
Figure 5. Time lapse infection of SARS-CoV-2 in VERO E6 cells with immunofluorescence for viral Spike protein and cellular cytoskeleton in 12 **(A)**, 16 **(B)**, 20 **(C)** and 24 **(D)** hpi**.** Immunofluorescence marking viral Spike (green) and cellular F-actin/cytoskeleton (magenta) in 12 **(A)**, 16 **(B)**, 20 **(C)** and 24 **(D)** hpi of VERO E6 cells, evidencing the high viral replication in 16 hpi and alterations in cellular morphology induced by SARS-CoV-2 **(C-D)**.

To better understand the nature of these MVB-like FISH and IF labeling observed, Spike IF was performed in VERO E6 cells infected with SARS-CoV-2 (MOI 1), using double IF labeling for various cellular organelles, especially those involved in autophagy and related pathways, to evaluate the interaction between the virus and cellular machinery. These organelles play different roles in cellular processes, such as endocytosis, protein trafficking, and degradation (*90, 91*). Double IF was performed to using known markers for: early endosomes (**Figure 6**)**,** involved in sorting and recycling internalized material (*92*); late endosomes (**Figure 7**), lysosomes (**Figure 8**) and autophagosome (**Figure 9**), responsible for the degradation of internalized and intracellular material (*93, 94*); cis-Golgi (**Figure 10**), responsible for receiving newly synthesized proteins from endoplasmic reticulum and initiating their maturation and trafficking throughout the Golgi network (*95*); and MVB (**Figure 11**), responsible for the degradation of specific membrane proteins and the secretion of exosomes (*96, 97*). These analyzes revealed a probable interaction of viral particles with endosomes (**Figure 6** and **Figure 7 C-D''**), autophagosome (**Figure 9**) and MVB (**Figure 11**), as described and discussed below.

During viral infection, autophagy can serve as a defense mechanism through xenophagy, degrading exogenous molecules (*98*). In this process, the phagophore engulfs the material to be degraded, forming the autophagosome, which subsequently fuses with lysosomes to form autolysosomes - the final step in the material's degradation (*99*). Autophagosomes can also fuse with endosomes, creating structures known as amphisomes (*98*), which may explain the presence of viral material in autophagosomes, endosomes, and MVBs. However, no colocalization of viral particles and Lamp-1, a lysosomal marker (*100*), was observed (**Figure 8 C-D''**), indicating that no lysosomal degradation of these viral particles was occurring.

A proximal, but not co-localized, marking of cis-Golgi and Spike (**Figure 10**) suggested a possible involvement of the region of endoplasmic-reticulum–Golgi intermediate compartment (ERGIC) in viral replication and/or egress. Some viruses, including CoVs, are known to induce the remodulation of cell membranes to favor replication, utilizing the endoplasmic reticulum, Golgi, and ERGIC as assembly and budding sites for structural particles like M, E, and N (*101–103*), as well as forming

double membrane vesicles (DMVs) that anchor the replication-transcription complexes (RTCs) (*104*, *105*).

CoVs generates a large number of isolated DMVs with an undefined origin, but they are likely derived from the ER, late endosomes, autophagosomes, or the secretory pathway. These DMVs tend to integrate into a unique reticulovesicular network of shaped ER membranes (*106*). This model of DMVs production and interaction with ERGIC has already been proposed for SARS-CoV-2, with probably role in evading the antiviral innate immune response (*107*). This could explain the presence of viral particles that are not co-localized with the cis-Golgi and the circular structures containing viral particles observed in various immunofluorescence images (**Figure 3**, **Figure 4** and **Figure 6**-**Figure 11**).

Figure 6. **Immunofluorescence analysis for the detection of viral Spike protein and early endosome in VERO E6 cells.** Immunofluorescence marking viral Spike (green) and early endosome (red - EEA1 antibody), evidencing the colocalization of viral particles and the organelle **(C'', D'')**.

Figure 7. **Immunofluorescence analysis for the detection of viral Spike protein and late endosome in VERO E6 cells.** Immunofluorescence marking viral Spike (green) and late endosome (red – CD63 antibody), evidencing the colocalization of viral particles and the organelle (**C''**, **D''**).
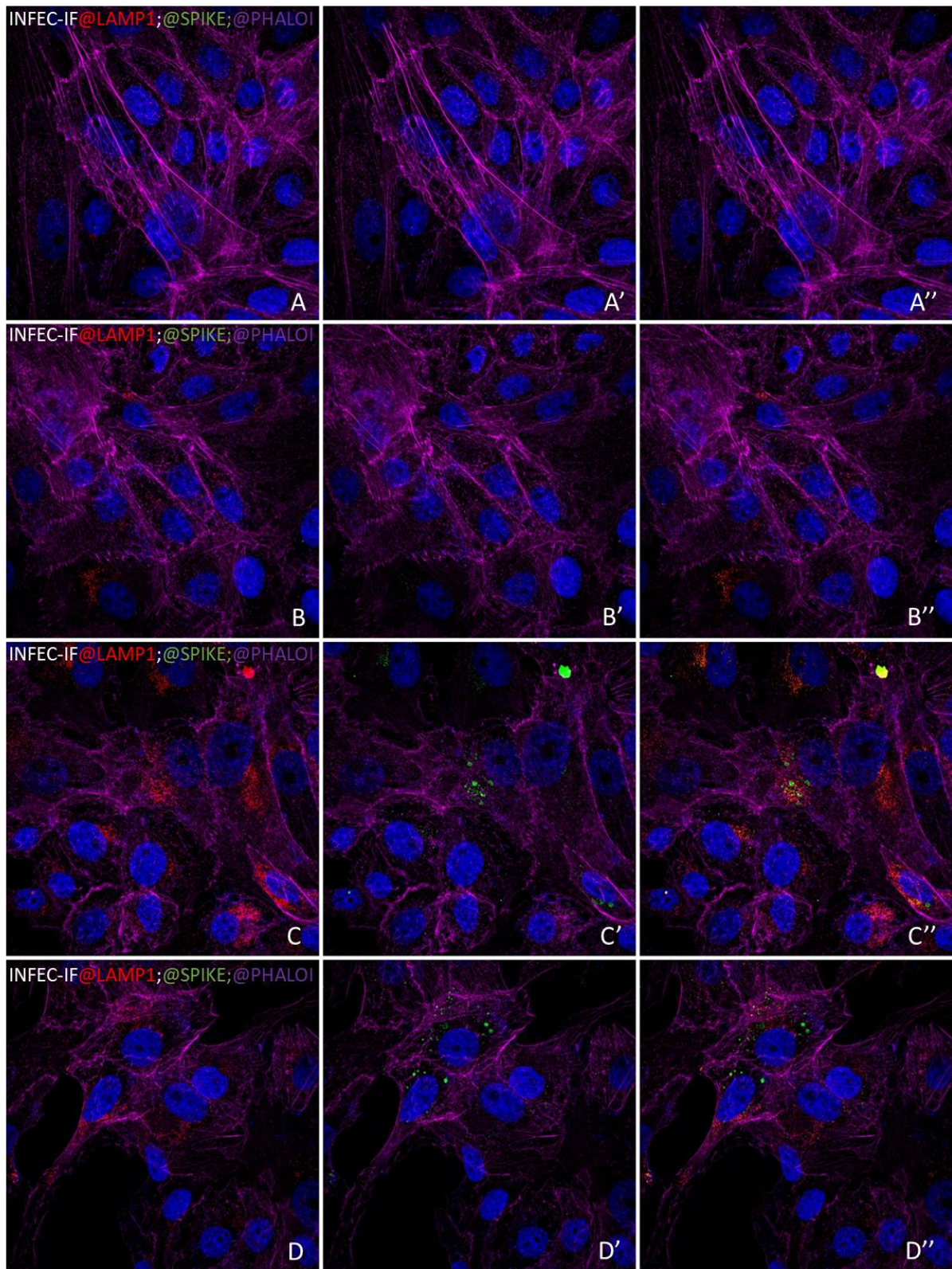
Figure 8. **Immunofluorescence analysis for the detection of viral Spike protein and lysosomes in VERO E6 cells.** Immunofluorescence marking viral Spike (green) and lysosomes (red – LAMP1 antibody), with no colocalization of viral particles and the organelle (**C''**, **D''**), with exception of the presence of technical artifacts.
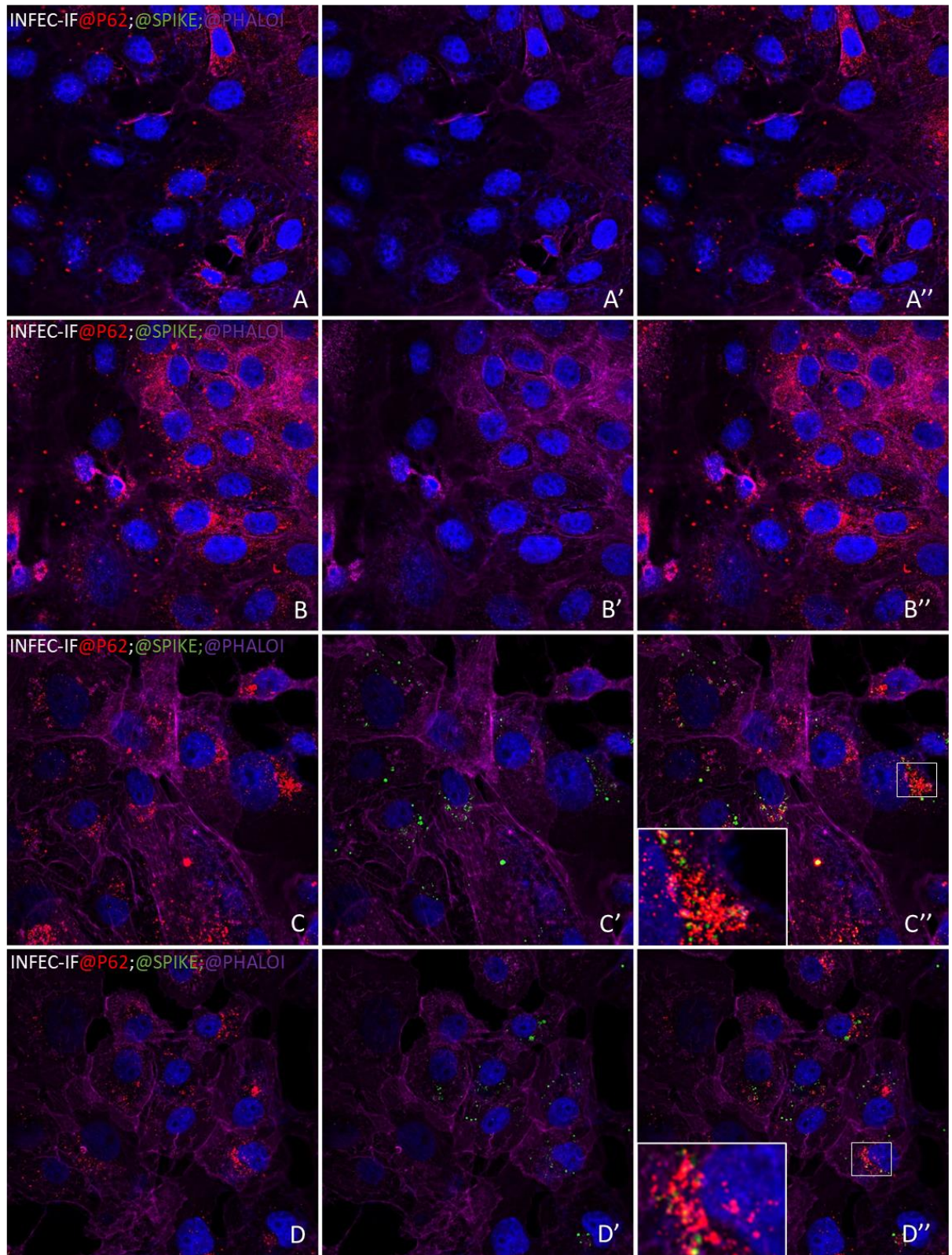
Figure 9. **Immunofluorescence analysis for the detection of viral Spike protein and autophagosomes in VERO E6 cells.** Immunofluorescence marking viral Spike (green) and autophagosomes (red – P62 antibody), with colocalization of viral particles and the organelle (**C''**, **D''**).
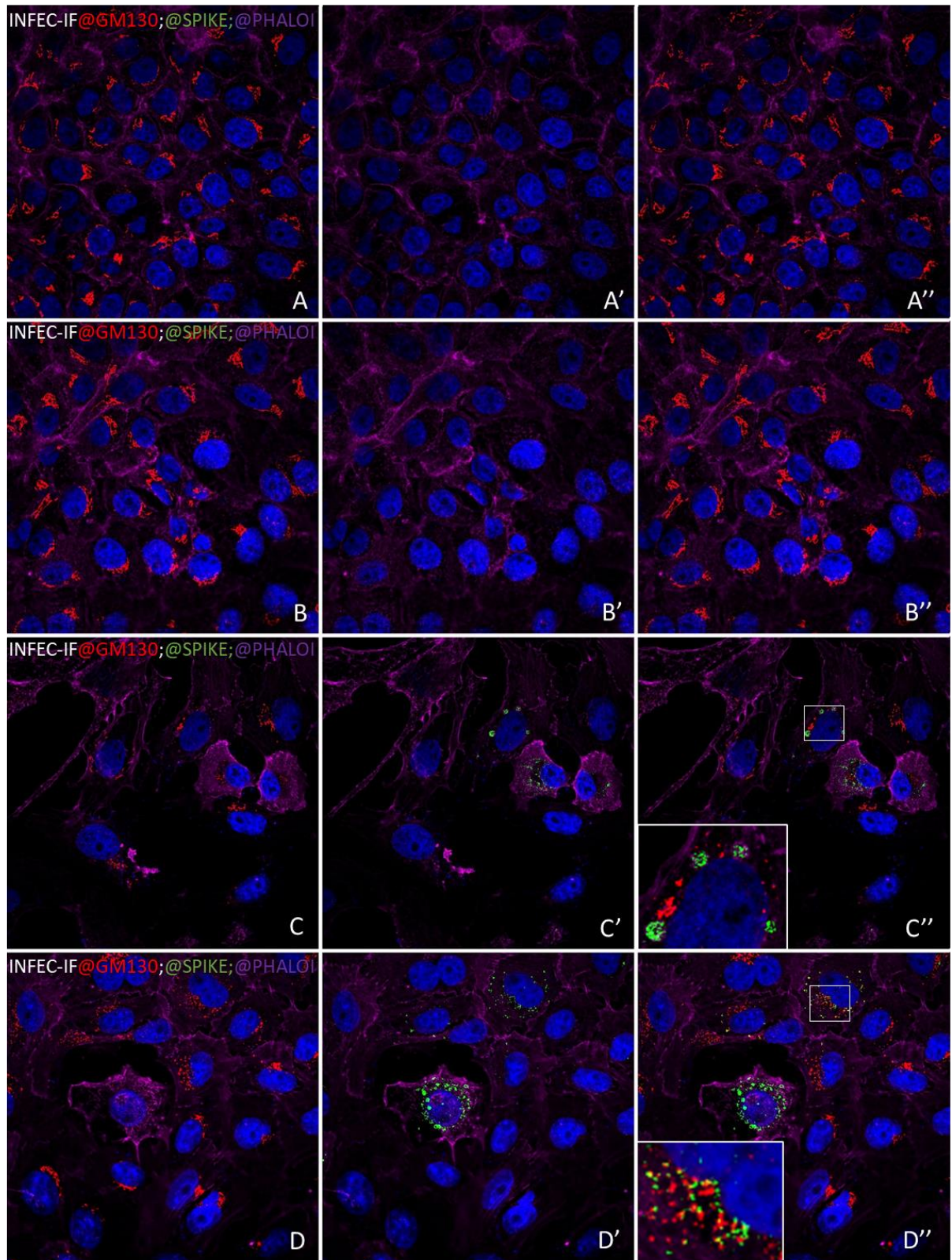
Figure 10. **Immunofluorescence analysis for the detection of viral Spike protein and cis-Golgi in VERO E6 cells.** Immunofluorescence marking viral Spike (green) and cis-Golgi (red – GM130 antibody), with no colocalization of viral particles and the organelle, but showing proximal interaction (**C''**, **D''**).
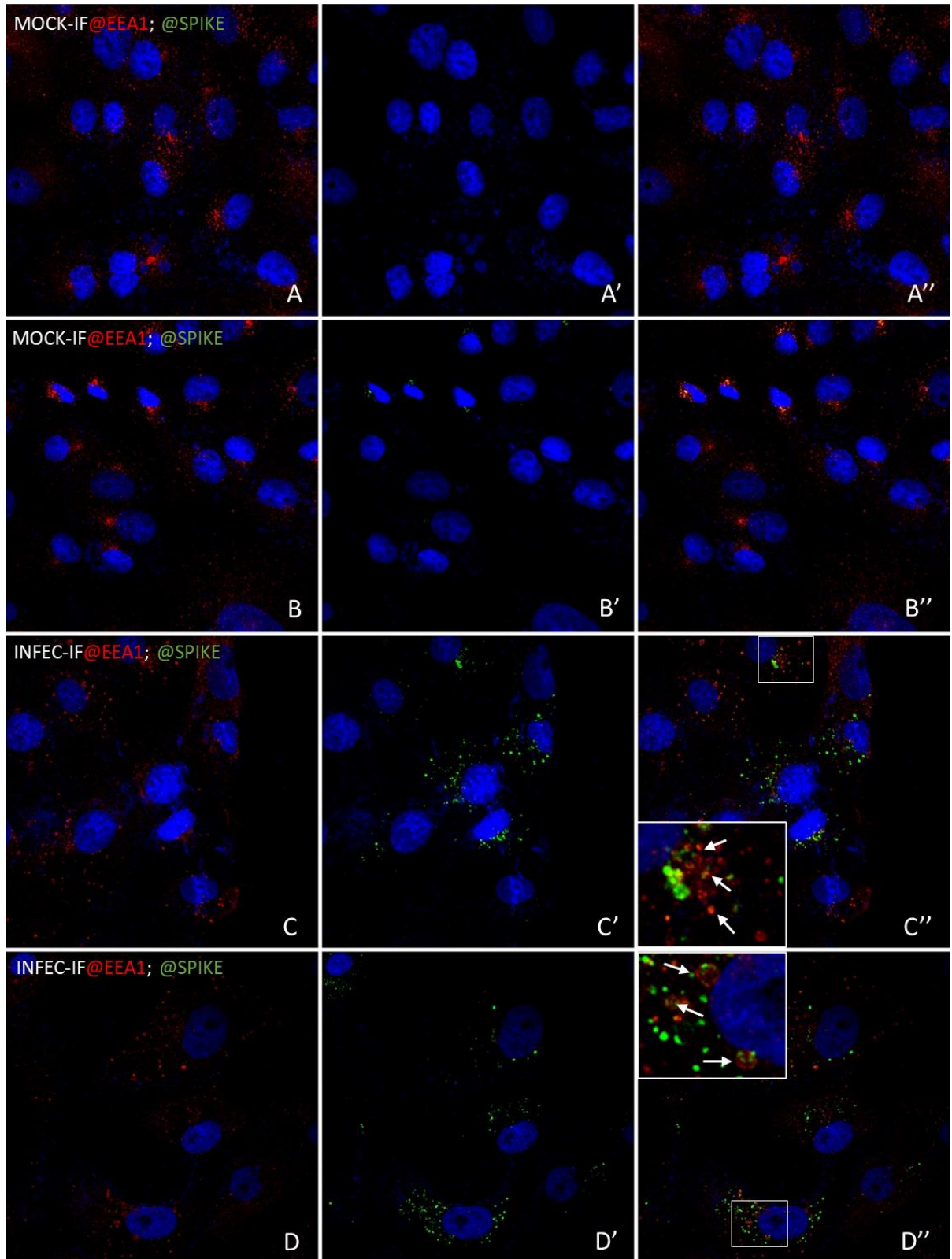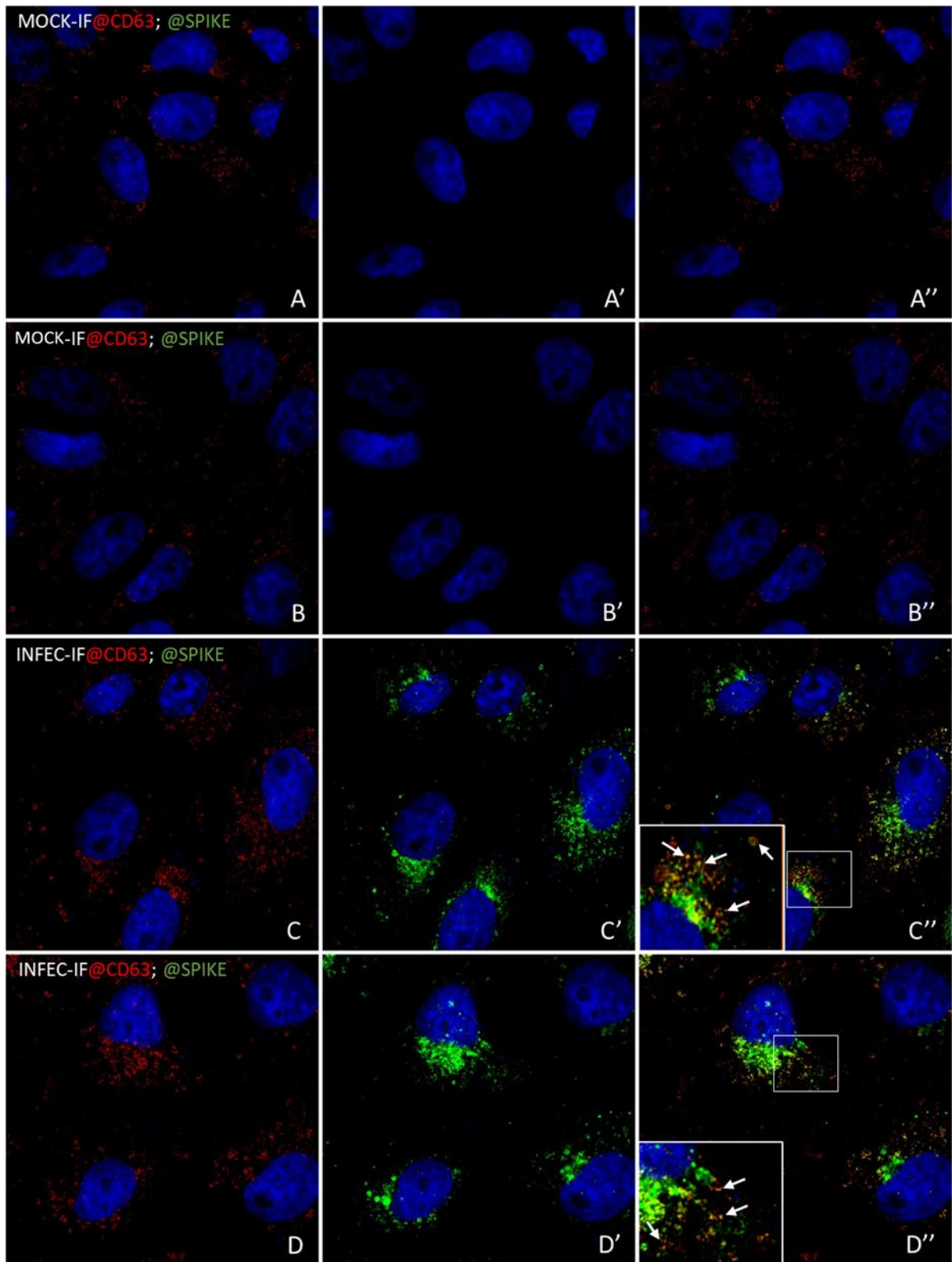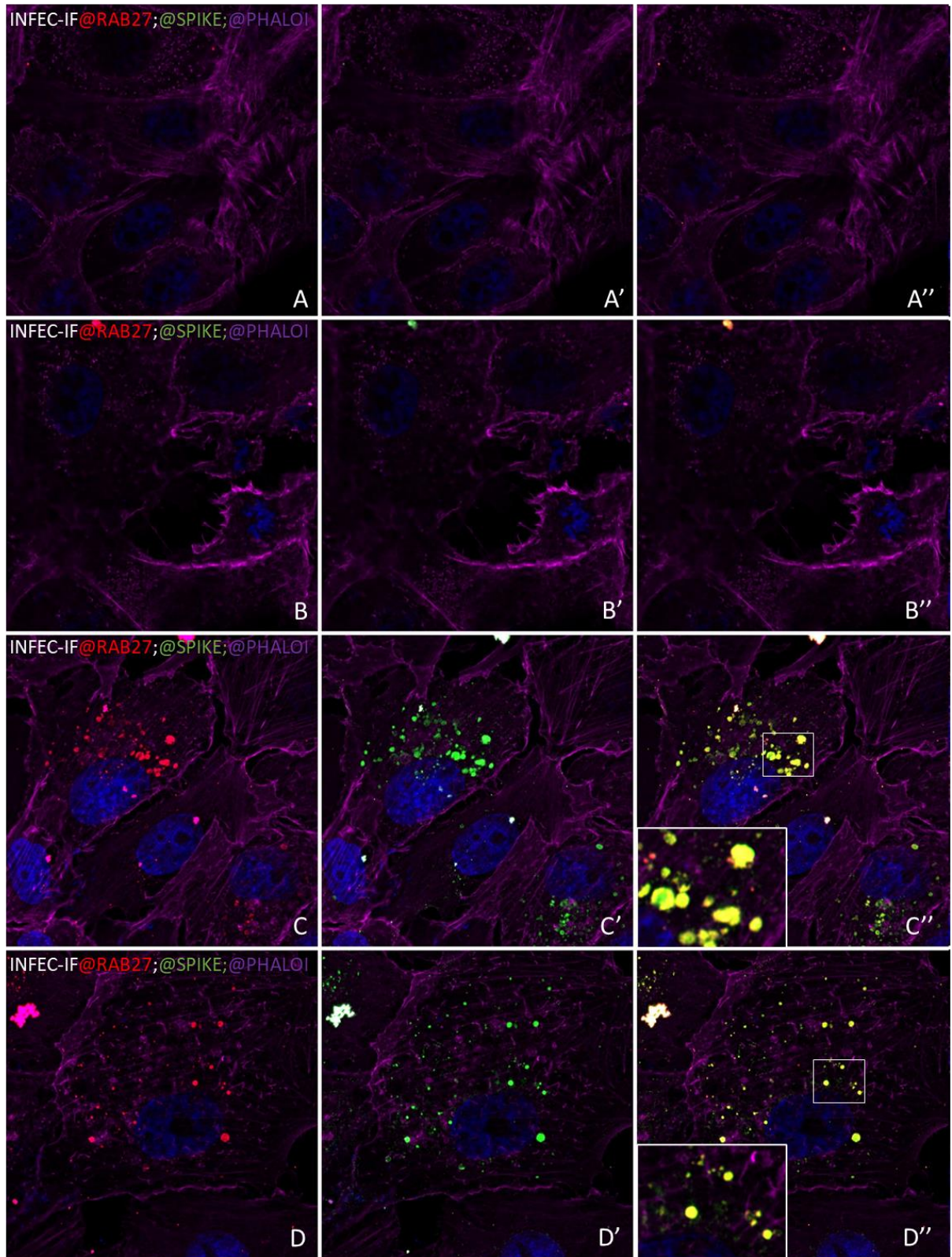
Figure 11. **Immunofluorescence analysis for the detection of viral Spike protein and multivesicular-bodies in VERO E6 cells.** Immunofluorescence marking viral Spike (green) and multivesicular bodies (red – RAB27 antibody), with colocalization of viral particles and the organelle (**C''**, **D''**).

It was also observed strong indicative on the occurrence of the phenomenon of cellular-cellular transference of viral particles through cellular membrane projections in VERO E6 cells, using both immunofluorescence and FISH techniques (**Figure 12**).

Diverse virus, including respiratory viruses, are capable of spreading in hosts through cell-to-cell contact, using mechanisms as nanotubes, fast lanes (*108*), filopodial bridges (*109*) and cell-cell fusion, resulting in a single giant and multinuclear cell, known as syncytium (*110*). Differently of membrane budding, the most common form of interhost spread infection in respiratory viruses, the spread through direct cell-to-cell, does not require the complete assembly of viral particles, allowing spreading of partially assembled viral particles, such as nucleocapsids and inclusion bodies (*108*).

We captured the presence of both filopodia containing viral RdRp mRNA using FISH (**Figure 12 A-C**), fast lanes using FISH and immunofluorescence (**Figure 12 E-H''**) and syncytia (**Figure 12 I**) using immunofluorescence (**Figure 12 E-H''**). It was also observed the presence of viral Spike double-stained with CD63 (**Figure 12 H''**), which demonstrating the presence of viral-containing late endosomes/MVBs in cell-to-cell connections.

No evidence of this type of spread was registered to SARS-CoV-2 until the moment of our observation. However, recently, the spread of SARS-CoV-2 through cell-to-cell transmission (*111*) and nanotubes tunneling (*112*) was reported, as well as syncytia formation (*111*), indicating that viral Spike protein mediates cell-to-cell contact. Additionally, it was observed that ACE2 is required for viral entry in host cell, but it is not necessary required for cell-to-cell transmission in SARS-CoV-2 infection, in opposite to SARS-CoV (*111*). The presence of similar viral vesicular structures and DMV was also reported to occur in nanotubes in VERO E6 cells (*112*), as here registered (**Figure 3**, **Figure 4**, **Figure 6** and **Figure 12**), and may provide a route for neural spread, enabling the spread of viruses from permissive to nonpermissive to infection cells.

FISH@RdRp · A

FISH@RdRp · B

FISH@RdRp · C

FISH@RdRp · D

FISH@RdRp · E

FISH@RdRp · F

FISH@RdRp · G

FISH@RdRp · F

IF@CD63 · G

IF@SARS-CoV-2 Spike · H

IF@CD63 · H'

Merge · H''

FISH@RdRp · I
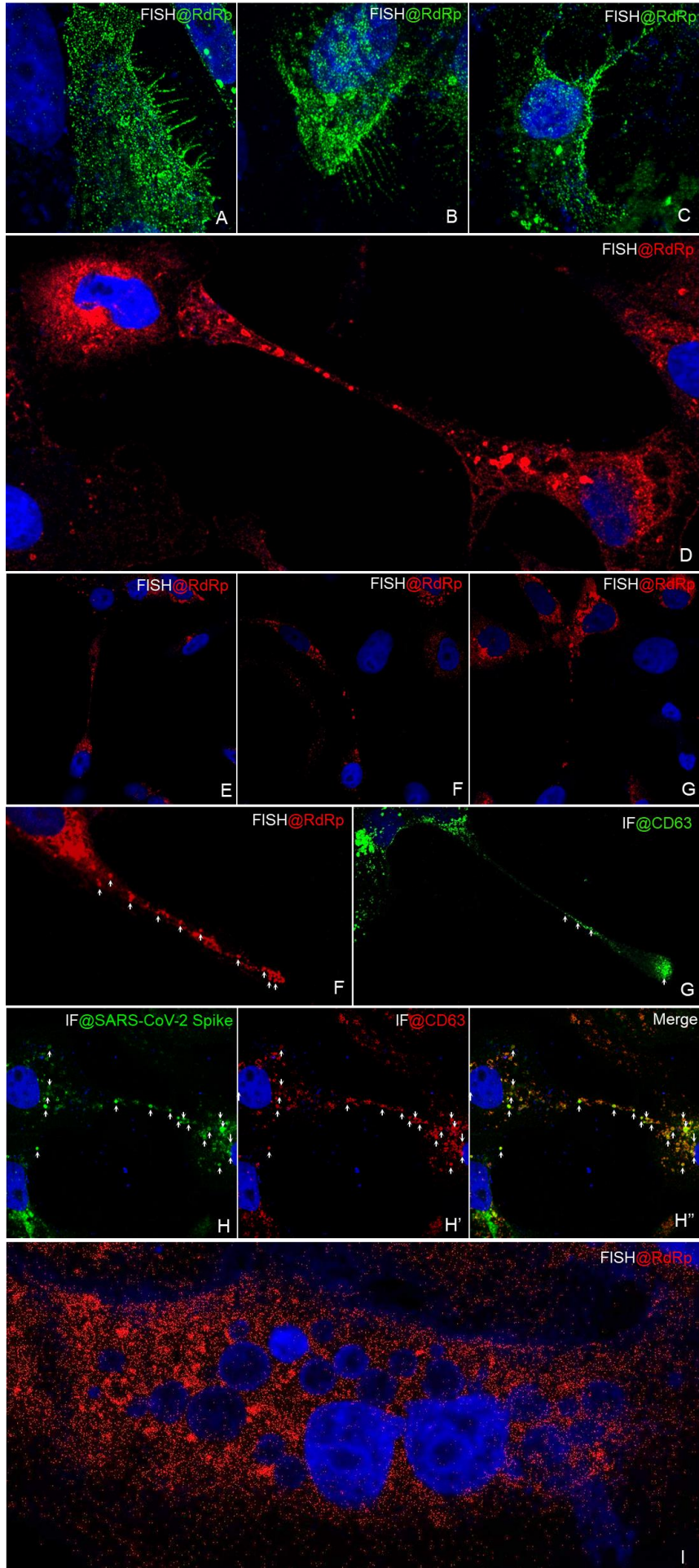
Figure 12. **Detection of SARS-CoV-2 particles in cell-to-cell connections of VERO E6 model cells using fluorescent in situ hybridization (A-F and I) and immunofluorescence (H) techniques.** Detection of SARS-CoV-2 RNA-dependent RNA polymerase gene by FISH in filopodia (**A-C**), structures in cell-to-cell connections (**D-F**) and syncytia (**I**). Immunofluorescence for Spike protein (**H**) co-stained with CD63 (**H'**), demonstrating the presence of viral-containing late endosomes/MVBs in cell-to-cell connections (**H''**).

It is known that some microorganisms can hijack autophagy, including xenophagy, by suppressing or triggering it (*113*), to promote their replication, survival, and egress (*114*), specially using autophagosomes (*115*) and endosomes (*116*). After starting the analysis of images from immunohistology technique, hypotheses were elaborated on the relationship between the phenomenon of cell autophagy and viral replication, as well as the occurrence of transfer of viral particles to neighboring cells via cell-cell contact. To partially confirm these hypotheses, we performed an RT-qPCR analysis to evaluate the expression of genes related to autophagy, cell death, and cytoskeleton remodeling. RT-qPCR was conducted on both VERO E6 and A549 cells due to the high susceptibility of VERO E6 cells to infection and the lower susceptibility of A549 cells, in order to investigate the impact of viral entry on target genes in cells with and without Ace-2 and SARS-CoV-2 abundance.

It was found that AMBRA-1 expression, one of the factors that initiates and regulates the autophagic response (*117*), was increased upon SARS-CoV-2 infection in both VERO and A549 cells (**Figure 13 A**, **A'**). The same phenomenon was observed for the autophagy genes ATG7, involved in elongation phase, and BECN1, involved in nucleation phase of autophagosome (*118*) (**Figure 13 B**, **C'**). In order to assess the fusion between the autophagosome and the lysosome, an important step in autophagic flux, we examined the expression of genes VAMP8 and SNAP29, which are crucial for autophagosome-lysosome fusion. SNAP29 acts mediating the fusion of STX17 present in autophagosome with VAMP8, present in lysosome membrane, forming the STX17-SNAP29-VAMP8-mediated autophagosome fusion complex (*119*). Interestingly, in VERO E6 cells, the one in which viral infection is highly significant, VAMP8 expression was very low in mock cells, requiring an increase in number of cycles in RT-qPCR reaction to obtain some detection, and it

showed a small reduction (no statistical significance) in infected cells (**Figure 13 D**). In A549, where a viral infection is weak, the expression of VAMP8 was highly increased in the infected cells (**Figure 13 D'**). In SNAP29 the gene expression was upregulated upon infection for both cellular types (**Figure 13 E**, **E'**). These results suggested that VAMP8, essential for autophagosome and lysosome fusion, may be down-regulated by the virus in VERO cells, and may explain the lower rate of viral success in infecting A549 cells, as the autophagosomes carrying viral particles are probably fused with lysosome, allowing its chemical digestion.

When evaluating the expression of the anti-apoptotic gene BCL-2 (*120*), a very significant increase was observed in VERO cells upon infection, while a significant increase, but lower compared to VERO E6, was detected in A549, suggesting inhibition of apoptosis in both cell types (**Figure 13 F** and **F'**). In addition to being an inhibitor of apoptosis, BCL-2 acts regulating negatively autophagy (*121*), which is counterintuitive to the concomitant increase of both BCL-2 and autophagy genes in both cell types. Interestingly, Ambra-1 also acts by binding to mitochondrial BCL-2, preventing its interaction with BECN1and thus allowing autophagy to occur (*122*). When compared the rate of elevation of AMBRA-1 in infected cells, we observed an apparently higher one in VERO compared to A549 (**Figure 13 A**, **A'**). These results suggest that, in VERO E6 cells, the up-regulation of autophagy genes could be promoting this process even in a condition of possible inhibition of apoptosis (high BCL-2), due to the excess increase of the AMBRA-1 gene.

Finally, we observed that, of the three target-genes involved in cytoskeletal remodeling, they all were induced by viral infection (**Figure 13 H-I'**). The only exception is the expression of RAC1 in A549 (**Figure 13 G**, **G'**), showing that, in VERO cells, this gene may be signaling a virus-induced phenomenon in robustly infected cells, with a possible role in cell-to-cell transmission of viral particles.
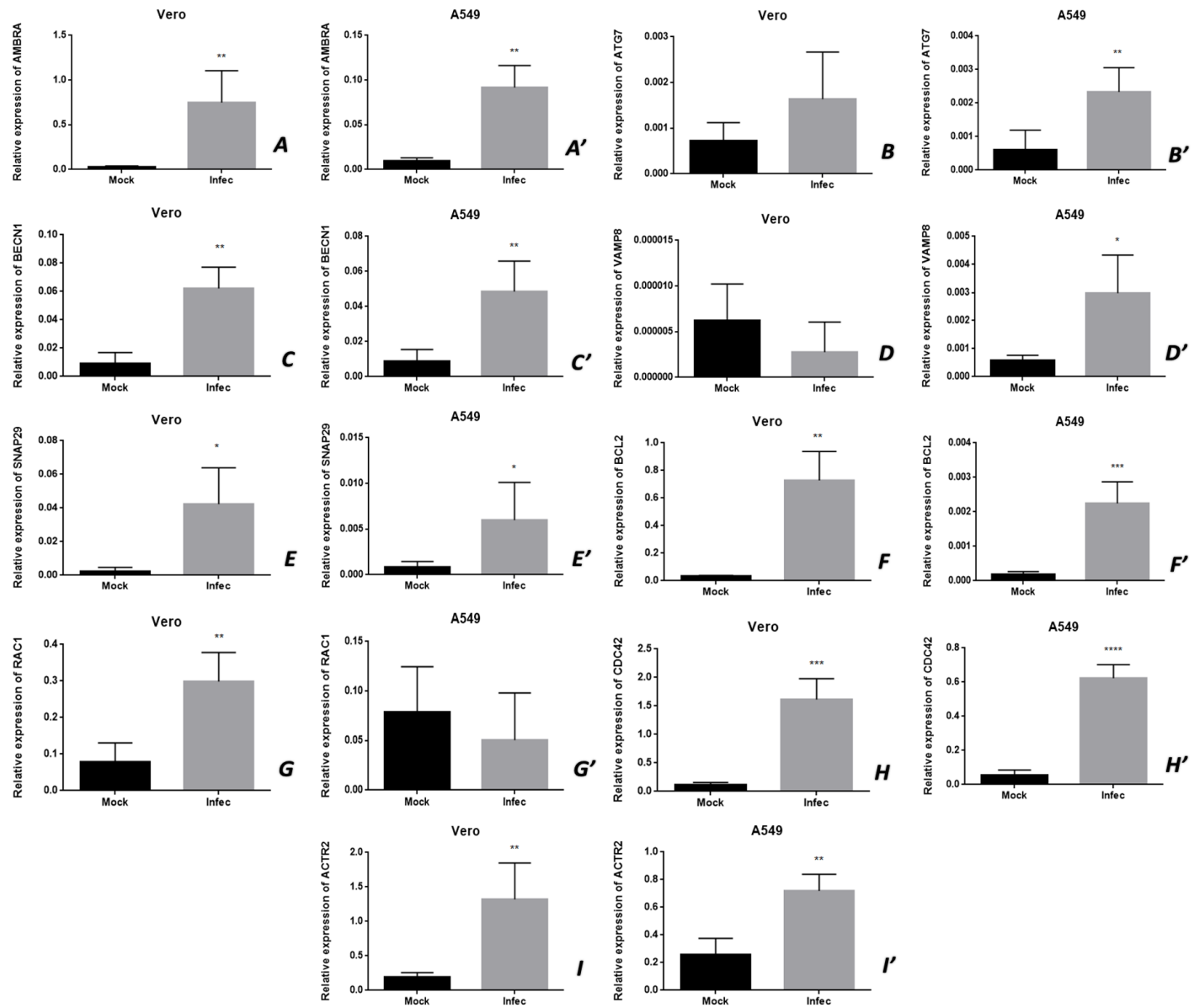
Figure 13. **RT-qPCR analysis of autophagy, apoptosis, and cytoskeleton remodeling genes in VERO E6 and A549 cells.** Expression of genes involved in autophagy pathway (**A-E**), apoptosis (**F**) and cytoskeletal remodulation (**G-I**) for both VERO E6 and A549 for mock and infect condition, showing an increase in almost all genes upon infection, with higher rate in VERO E6, except for VAMP8 gene for VERO E6 (**D**) and RAC1 in A549 (**G'**). No statistical significance for ATG7 in VERO E6 (**B**).

The results obtained with RT-qPCR showed up-regulation of autophagy genes and a decrease in the autophagosome-lysosome fusion gene VAMP8 (**Figure 13**), corroborating the results of immunofluorescence, in which endosomes (**Figure 6** and **Figure 7 C-D''**), autophagosomes (**Figure 9**) and MVBs (**Figure 11**) showed colocalization with viral particles, while no colocalization was detected for lysosomal marker Lamp-1 (**Figure 8C-D''**). This data strongly suggested that, although autophagy was active in infected VERO E6 cells, no lysosomal degradation of these viral particles was occurring.

Additionally to its crucial role in promoting autophagosome-lysosome fusion, VAMP8 is also reported as an essential SNARE in regulation of exocytosis of mucin granule (*123*), exocrine glands (*124*, *125*), platelets (*126*), macrophages (*127*) and mast cells (*128*), as well as in the fusion of endosome and secretory vesicle fusion with the plasma membrane (*129–131*). As this gene was downregulated in infected VERO E6 cells, it was hypothesized that SARS-CoV-2 infection could possibly cause the blockage of exocytosis, reducing viral release. To confirm it, a PFU (plaque-forming units) assay was performed.

The amount of viable SARS-CoV-2 particles within VERO E6 cells was compared to the number of PFUs in present in extracellular compartment at 24 hpi (**Figure 14**). PFU assay resulted in the detection of 20-fold increase in the number of viable SARS-CoV-2 particles inside the VERO E6 cells compared to the supernatant at 8 hpi. Similarly, at 24 hpi, the number of viral particles retained inside the cells was 25 times higher than in the supernatant (**Figure 14 A**). In sharp contrast to SARS-CoV-2, the virus responsible for the 2003 SARS epidemic, SARS-CoV, demonstrated only a 10-fold increase in the number of viral particles present in supernatant as compared to inside the cells at 12 hpi in VERO E6 cells (*132*).

The observed repression of exocytosis-related gene VAMP8, combined with the findings of increased viral particles retained inside the infected cells, suggests that this phenomenon could be caused by hindered exocytosis. To verify this hypothesis, VERO E6 cells infected with SARS-CoV-2 were treated with the exocytosis-inducer bafilomycin (*133*). Surprisingly, bafilomycin treatment did not significantly affect the number of SARS-CoV-2 particles inside the cells (**Figure 14 B**). However, a substantial increase in viral particles was detected in the supernatant of the treated cells (**Figure 14 C**) suggesting that inhibition of exocytosis limits viral release to the extracellular medium during SARS-CoV-2 infection. These results offer valuable insights into the pathogenesis of SARS-CoV-2 and could provide potential targets for therapeutic interventions.
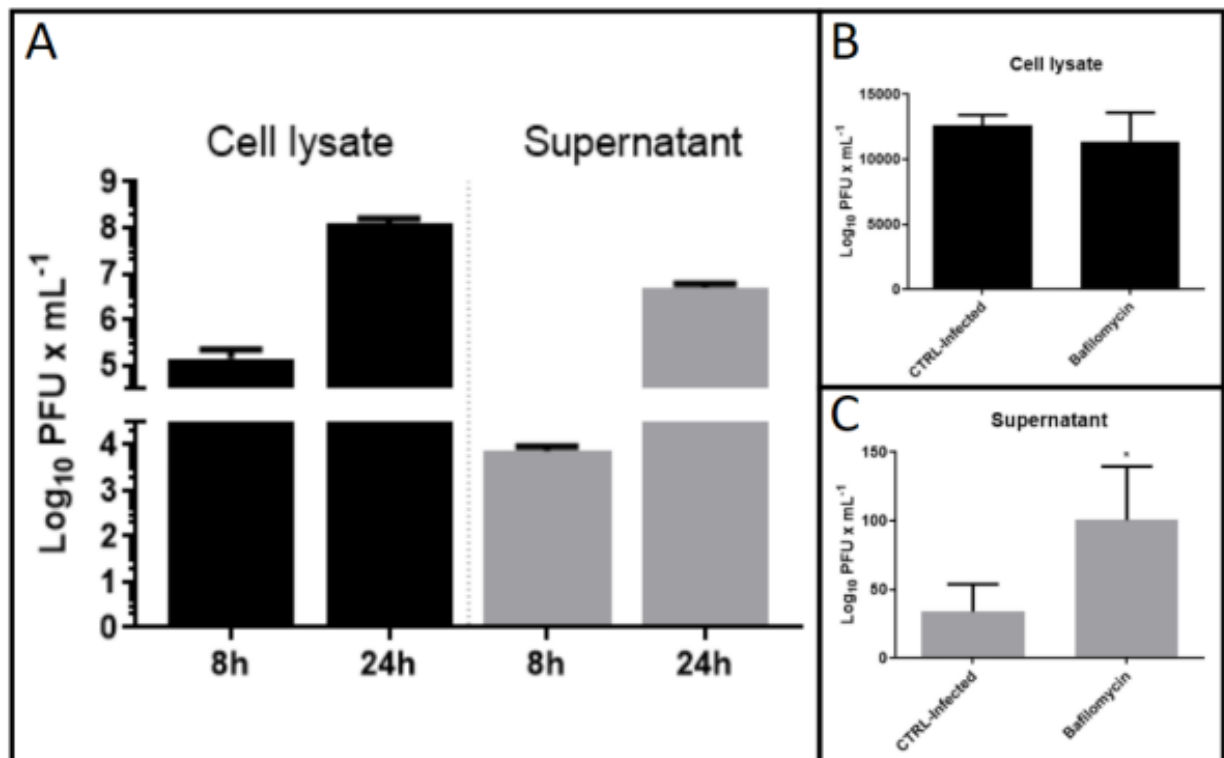
Figure 14. **PFU and Bafilomycin treatment 24 hpi in VERO E6 cells.** Focus forming assay of cell lysate and supernatant of VERO E6 cell culture 8 and 24 hpi with SARS-CoV-2. (**A**). RT-qPCR of cell lysate and (C) supernatant of VERO E6 cell culture treated with bafilomycin after 24 hpi with SARS-CoV-2. Bars represent mean ± SEM. Statistic difference is indicated by *p<0.05 (**B**).

CONCLUSION

The results obtained in this work strongly suggests the capacity of SARS-CoV-2 induces transcriptional activation of autophagy and repression of genes associated to lysosomes-vesicle fusion in VERO E6 cells, as was demonstrated by up-regulation of autophagy-related genes AMBRA-1, ATG7, BECN-1 and SNAP29 and downregulation of VAMP8 gene in RT-qPCR assay (**Figure 13**). Furthermore, it is demonstrated that newly assembled viral particles tend to accumulated within MVBs/late endosomes and autophagosomes upon SARS-CoV-2 infection (**Figure 6**, **Figure 7**, **Figure 9** and **Figure 11**), as it cannot be targeted to lysosomal degradation (**Figure 8** and **Figure 13**).

The increased expression of the antiapoptotic gene BCL-2, genes associated to cytoskeleton remodulation such as RAC1 (**Figure 13**) and the strong evidence of inhibition of exocytosis (**Figure 14**), associated to the visual evidence of colocalization of viral particles with autophagy-related organelles, suggests that blockage of autophagy flux is involved in viral replication, protection against immune detection and viral spread through cell-cell contact (**Figure 12**), using endosomes as vehicle (**Figure 15**), as it was possible to detected CD63-positive vesicles fulfilled with viral particles in cell-to-cell connections (**Figure 12 H''**). This hypothesis is also corroborated by Zeng et al. (2021), which showed that, in SARS-CoV-2, endosomal entry pathway is involved in cell-to-cell transmission.
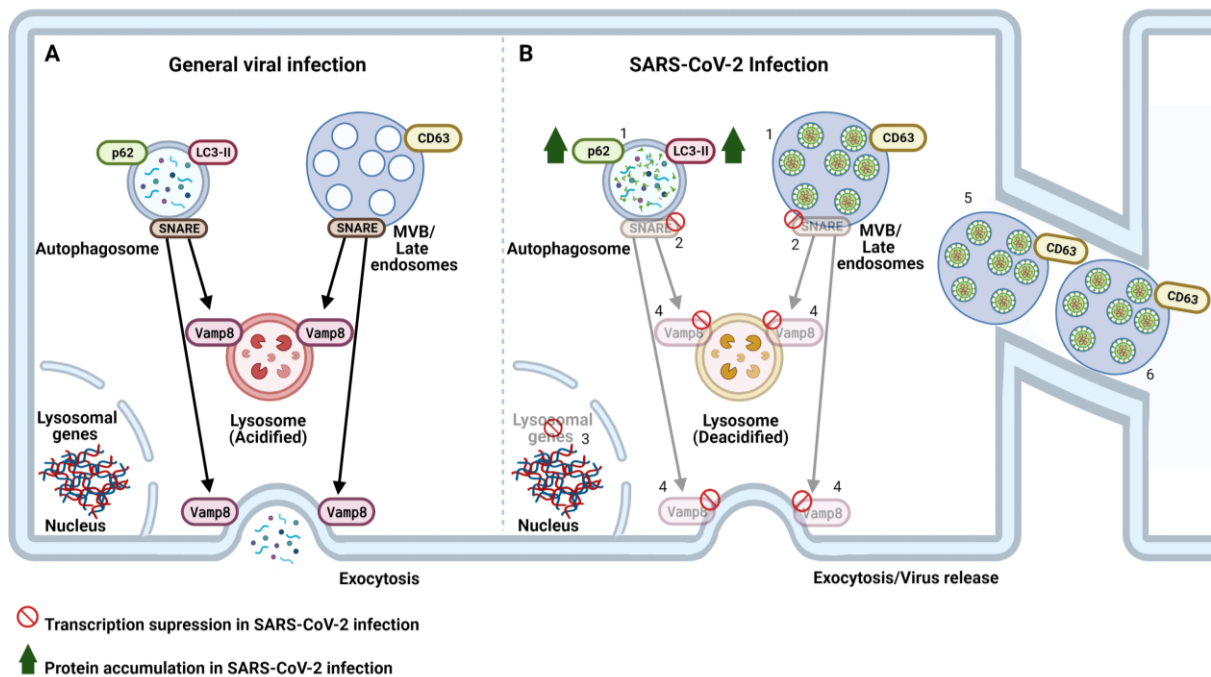
Figure 15. **Proposition of molecular mechanisms underlying SARS-CoV-2 infection and its involvement in compromising autophagy flux and vesicle fusion.** Scheme representing the classical autophagy flux upon general viral infection (**A**) and upon SARS-CoV-2 infection (**B**). Usually, SNARE proteins enable the fusion of vesicles with acidified lysosomes and to the cell membrane (**A**). In the scenario of SARS-CoV-2 infection, newly assembled viral particles associate with cellular vesicles (**1**) and are prevented from being degraded by enzymes during lysosomal fusion through modulation of the expression of genes that code for both vesicle fusion proteins (**2**) and lysosomal genes (**3**), causing lysosomal deacidification (**4**) and preventing lysosomal fusion with virus-bearing vesicles (**2, 4**). The repression of vesicle-membrane fusion proteins, such as VAMP8 (**4**), could prevent viral release from infected cells, causing accumulation of viral particles in MVBs (**5**), as observed in cell-to-cell connections (**6**). Created with BioRender.com

Additionally, the use of incomplete autophagy flux could explain why, in contrast to other coronaviruses (*134–137*), the use of drugs based in inhibition of autophagy, such as chloroquine (*138*) do not block infection by SARS-CoV-2 (*139*). As chloroquine inhibits the autophagic flux by blockage of autophagosomes-lysosomes binding (*138*, *140*), and evidences here shown suggests that impaired autophagy flux increase SARS-Cov-2 replication and spread, it is possible to conclude that blockage of complete autophagy flux by preventing autophagosomes-lysosomes binding is beneficial to propitiate viral infection, explaining why human

clinical trials using these drugs failed in establish its use as an effective treatment (*141–143*).

FINAL CONSIDERATIONS

The findings presented in this study, along with other simultaneously investigations worldwide, strongly suggest that SARS-CoV-2 infection may induce the activation of autophagy and repression of genes involved in lysosomal degradation and vesicle fusion, leading to the accumulation of viral particles in autophagosomes and MVBs/late endosomes. This phenomenon may account for the inefficacy of autophagy-inhibiting drugs against SARS-CoV-2 infection, unlike other coronaviruses. Moreover, the involvement of endosomes in cell-to-cell transmission of the virus, as shown by this and others studies, highlights the complexity of the mechanisms underlying SARS-CoV-2 replication and spread.

Additionally, it is well-known that mTOR plays a crucial role in regulating autophagy, as activation of mTOR signaling inhibits autophagy and its suppression promotes autophagy. The results here discussed regarding autophagy, along with recent evidence indicating increased mTOR signaling upon SARS-CoV-2 infection and its involvement in viral replication and spread via autophagy inhibition (*144, 145*), provide valuable insights into the biology of SARS-CoV-2 and may contribute to the development of more effective treatments and therapies for COVID-19, and also support the hypothesis of a possible relationship between autophagy, exercise, and fasting in preventing severe symptoms of SARS-CoV-2 infection through mTOR inactivation.

REFERENCES

1. F. Rohwer, D. Prangishvili, D. Lindell, Roles of viruses in the environment. *Environ. Microbiol.* **11**, 2771–2774 (2009).
2. K. Points, K. Terms, 9 . 3D : Medical Importance of Viruses, 2–4 (2021).
3. "Overview of Viruses and Virus Infection."
4. G. Luo, S. J. Gao, Global health concerns stirred by emerging viral infections. *J. Med. Virol.* **92**, 399–400 (2020).
5. F. W. Denny, The Clinical Impact of Human Respiratory Virus Infections. *Am. J. Respir. Crit. Care Med.* **152**, S4–S12 (1995).
6. C. S. Stover, C. M. Litwin, The Epidemiology of Upper Respiratory Infections at a Tertiary Care Center: Prevalence, Seasonality, and Clinical Symptoms. *J. Respir. Med.* **2014**, 1–8 (2014).
7. S. Rao, A. C. Nyquist, Respiratory viruses and their impact in healthcare. *Curr. Opin. Infect. Dis.* **27**, 342–347 (2014).
8. Z. Zhu, X. Lian, X. Su, W. Wu, G. A. Marraro, Y. Zeng, From SARS and MERS to COVID-19: A brief summary and comparison of severe acute respiratory infections caused by three highly pathogenic human coronaviruses. *Respir. Res.* **21** (2020), pp. 1–14.
9. H. J. Maier, E. Bickerton, P. Britton, Coronaviruses: Methods and protocols. *Coronaviruses Methods Protoc.* **1282**, 1–282 (2015).
10. V. C. C. Cheng, S. K. P. Lau, P. C. Y. Woo, Y. Y. Kwok, Severe acute respiratory syndrome coronavirus as an agent of emerging and reemerging infection. *Clin. Microbiol. Rev.* (2007), , doi:10.1128/CMR.00023-07.
11. T. Hu, Y. Liu, M. Zhao, Q. Zhuang, L. Xu, Q. He, A comparison of COVID-19, SARS and MERS. *PeerJ.* **8** (2020), doi:10.7717/peerj.9725.
12. J. Zheng, SARS-coV-2: An emerging coronavirus that causes a global threat. *Int. J. Biol. Sci.* **16**, 1678–1685 (2020).
13. C. M. Coleman, M. B. Frieman, Coronaviruses: Important Emerging Human Pathogens. *J. Virol.* **88**, 5209–5212 (2014).
14. R. M. Lana, F. C. Coelho, M. F. Da Costa Gomes, O. G. Cruz, L. S. Bastos, D. A. M. Villela, C. T. Codeço, The novel coronavirus (SARS-CoV-2) emergency and the role of timely and effective national health surveillance. *Cad. Saude Publica.* **36** (2020), doi:10.1590/0102-311x00019620.
15. K. G. Andersen, A. Rambaut, W. I. Lipkin, E. C. Holmes, R. F. Garry, The proximal origin of SARS-CoV-2. *Nat. Med.* **26**, 450–452 (2020).
16. COVID Live - Coronavirus Statistics - Worldometer, (available at https://www.worldometers.info/coronavirus/).
17. L. F. M Rezende I, B. I. Thome, M. I. Cabral Schveitzer, P. I. Roberto Borges de Souza-Júnior, C. I. Landmann Szwarcwald, L. F. M Rezende, Adults at high-risk of severe coronavirus disease-2019 (Covid-19) in Brazil, doi:10.11606/s1518-8787.2020054002596.
18. A. Booth, A. B. Reed, S. Ponzo, A. Yassaee, M. Aral, D. Plans, A. Labrique, D. Mohan, Population risk factors for severe disease and mortality in COVID-19: A global systematic review and meta-analysis. *PLoS One.* **16** (2021), p. e0247461.
19. L. Piroth, J. Cottenet, A. S. Mariet, P. Bonniaud, M. Blot, P. Tubert-Bitter, C. Quantin, Comparison of the characteristics, morbidity, and mortality of COVID-19 and seasonal influenza: a nationwide, population-based retrospective cohort study. *Lancet Respir. Med.* **9**, 251–259 (2021).

20. L. Lu, W. Zhong, Z. Bian, Z. Li, K. Zhang, B. Liang, Y. Zhong, M. Hu, L. Lin, J. Liu, X. Lin, Y. Huang, J. Jiang, X. Yang, X. Zhang, Z. Huang, A comparison of mortality-related risk factors of COVID-19, SARS, and MERS: A systematic review and meta-analysis. *J. Infect.* **81** (2020), pp. e18–e25.

21. O. A. Espinosa, F. Antunes, F. G. Longhi, P. F. Battaglini, Original article, 1–13 (2020).

22. M. Y. Wang, R. Zhao, L. J. Gao, X. F. Gao, D. P. Wang, J. M. Cao, SARS-CoV-2: Structure, Biology, and Structure-Based Therapeutics Development. *Front. Cell. Infect. Microbiol.* **10** (2020), , doi:10.3389/fcimb.2020.587269.

23. Y. Huang, C. Yang, X. feng Xu, W. Xu, S. wen Liu, Structural and functional properties of SARS-CoV-2 spike protein: potential antivirus drug development for COVID-19. *Acta Pharmacol. Sin.* **41** (2020), pp. 1141–1149.

24. J. Cui, F. Li, Z. L. Shi, Origin and evolution of pathogenic coronaviruses. *Nat. Rev. Microbiol.* **17** (2019), pp. 181–192.

25. N. Petrosillo, G. Viceconte, O. Ergonul, G. Ippolito, E. Petersen, Narrative review COVID-19, SARS and MERS: are they closely related? *Clin Microbiol Infect.* **26**, 729 (2020).

26. Y. Song, M. Zhang, L. Yin, K. Wang, Y. Zhou, M. Zhou, Y. Lu, COVID-19 treatment: close to a cure? A rapid review of pharmacotherapies for the novel coronavirus (SARS-CoV-2). *Int. J. Antimicrob. Agents.* **56** (2020), , doi:10.1016/j.ijantimicag.2020.106080.

27. WHO Coronavirus (COVID-19) Dashboard | WHO Coronavirus (COVID-19) Dashboard With Vaccination Data, (available at https://covid19.who.int/).

28. WHO EMRO | MERS outbreaks | MERS-CoV | Health topics, (available at http://www.emro.who.int/health-topics/mers-cov/mers-outbreaks.html).

29. E. Mahase, Coronavirus covid-19 has killed more people than SARS and MERS combined, despite lower case fatality rate. *BMJ.* **368**, m641 (2020).

30. T. M. Abdelghany, M. Ganash, M. M. Bakri, H. Qanash, A. M. H. Al-Rajhi, N. I. Elhussieny, SARS-CoV-2, the other face to SARS-CoV and MERS-CoV: Future predictions. *Biomed. J.* **44**, 86–93 (2021).

31. A. E. Benefield, L. A. Skrip, A. Clement, R. A. Althouse, S. Chang, B. M. Althouse, SARS-CoV-2 viral load peaks prior to symptom onset: A systematic review and individual-pooled analysis of coronavirus viral load from 66 studies. *medRxiv* (2020), doi:10.1101/2020.09.28.20202028.

32. L. Zou, F. Ruan, M. Huang, L. Liang, H. Huang, Z. Hong, J. Yu, M. Kang, Y. Song, J. Xia, Q. Guo, T. Song, J. He, H.-L. Yen, M. Peiris, J. Wu, SARS-CoV-2 Viral Load in Upper Respiratory Specimens of Infected Patients. *N. Engl. J. Med.* **382**, 1177–1179 (2020).

33. T. Singhal, A Review of Coronavirus Disease-2019 (COVID-19). *Indian J. Pediatr.* **87**, 281–286 (2020).

34. N. G. Davies, P. Klepac, Y. Liu, K. Prem, M. Jit, C. A. B. Pearson, B. J. Quilty, A. J. Kucharski, H. Gibbs, S. Clifford, A. Gimma, K. van Zandvoort, J. D. Munday, C. Diamond, W. J. Edmunds, R. M. G. J. Houben, J. Hellewell, T. W. Russell, S. Abbott, S. Funk, N. I. Bosse, Y. F. Sun, S. Flasche, A. Rosello, C. I. Jarvis, R. M. Eggo, Age-dependent effects in the transmission and control of COVID-19 epidemics. *Nat. Med.* **26**, 1205–1211 (2020).

35. O. A. Espinosa, A. D. S. Zanetti, E. F. Antunes, F. G. Longhi, T. A. de Matos, P. F. Battaglini, Prevalence of medical conditions in patients and mortality cases affected by SARS-CoV2: A systematic review and meta-analysis. *Rev. Inst. Med. Trop. Sao Paulo.* **62**, 1–13 (2020).

36. A. Sanyaolu, C. Okorie, A. Marinkovic, R. Patidar, K. Younis, P. Desai, Z. Hosein, I. Padda, J. Mangat, M. Altaf, Comorbidity and its Impact on Patients with COVID-19. *SN Compr. Clin. Med.* **2**, 1069–1076 (2020).

37. G. Das, B. V. Shravage, E. H. Baehrecke, Regulation and function of autophagy during cell survival and cell death. *Cold Spring Harb. Perspect. Biol.* **4**, 1–14 (2012).

38. K. Jing, K. Lim, Why is autophagy important in human diseases? *Exp. Mol. Med.* **44**, 69–72 (2012).

39. P. Codogno, A. J. Meijer, Autophagy and signaling: Their role in cell survival and cell death. *Cell Death Differ.* **12** (2005), pp. 1509–1518.

40. Y. C. Kim, K. L. Guan, MTOR: A pharmacologic target for autophagy regulation. *J. Clin. Invest.* **125**, 25–32 (2015).

41. W. W. Y. Yim, N. Mizushima, Lysosome biology in autophagy. *Cell Discov.* **6** (2020), p. 6.

42. Y. Xu, N. T. Eissa, Autophagy in innate and adaptive immunity. *Proc. Am. Thorac. Soc.* **7**, 22–28 (2010).

43. K. Mao, D. J. Klionsky, Xenophagy: A battlefield between host and microbe, and a possible avenue for cancer treatment. *Autophagy.* **13**, 223 (2017).

44. D. Benvenuto, S. Angeletti, M. Giovanetti, M. Bianchi, S. Pascarella, R. Cauda, M. Ciccozzi, A. Cassone, Evolutionary analysis of SARS-CoV-2: how mutation of Non-Structural Protein 6 (NSP6) could affect viral autophagy. *J. Infect.* **81** (2020), doi:10.1016/j.jinf.2020.03.058.

45. C.-S. Shi, H.-Y. Qi, C. Boularan, N.-N. Huang, M. Abu-Asab, J. H. Shelhamer, J. H. Kehrl, SARS-Coronavirus Open Reading Frame-9b Suppresses Innate Immunity by Targeting Mitochondria and the MAVS/TRAF3/TRAF6 Signalosome. *J. Immunol.* **193** (2014), doi:10.4049/jimmunol.1303196.

46. A. Abdoli, M. Alirezaei, P. Mehrbod, F. Forouzanfar, Autophagy: The multi-purpose bridge in viral infections and host cells. *Rev. Med. Virol.* **28** (2018), , doi:10.1002/rmv.1973.

47. Y. Honma, K. Miyagawa, Y. Hara, T. Hayashi, M. Kusanaga, N. Ogino, S. Minami, S. Oe, M. Ikeda, K. Hino, M. Harada, Correlation of hepatitis C virus-mediated endoplasmic reticulum stress with autophagic flux impairment and hepatocarcinogenesis. *Med. Mol. Morphol.* (2021), doi:10.1007/s00795-020-00271-5.

48. S. Das, C. St. Croix, M. Good, J. Chen, J. Zhao, S. Hu, M. Ross, M. M. Myerburg, J. M. Pilewski, J. Williams, S. E. Wenzel, J. K. Kolls, A. Ray, P. Ray, Interleukin-22 Inhibits Respiratory Syncytial Virus Production by Blocking Virus-Mediated Subversion of Cellular Autophagy. *iScience.* **23**, 101256 (2020).

49. S. Maity, A. Saha, Therapeutic Potential of Exploiting Autophagy Cascade Against Coronavirus Infection. *Front. Microbiol.* **12**, 1173 (2021).

50. X. Dai, O. Hakizimana, X. Zhang, A. C. Kaushik, J. Zhang, Orchestrated efforts on host network hijacking: Processes governing virus replication. *Virulence.* **11** (2020), pp. 183–198.

51. S. E. Crawford, J. M. Hyser, B. Utama, M. K. Estes, Autophagy hijacked through viroporin-activated calcium/calmodulin-dependent kinase kinase-β signaling is required for rotavirus replication. *Proc. Natl. Acad. Sci. U. S. A.* **109**, E3405–E3413 (2012).

52. J. Y. Kim, L. Wang, J. Lee, J. J. Ou, Hepatitis C Virus Induces the Localization of Lipid Rafts to Autophagosomes for Its RNA Replication. *J. Virol.* **91** (2017), doi:10.1128/jvi.00541-17.

53. D. Ploen, E. Hildt, Hepatitis C virus comes for dinner: How the hepatitis C virus interferes with autophagy. *World J. Gastroenterol.* **21**, 8492–8507 (2015).

54. W. T. Jackson, T. H. Giddings, M. P. Taylor, S. Mulinyawe, M. Rabinovitch, R. R. Kopito, K. Kirkegaard, Subversion of cellular autophagosomal machinery by RNA viruses. *PLoS Biol.* **3** (2005), doi:10.1371/journal.pbio.0030156.

55. A. L. Richards, W. T. Jackson, How Positive-Strand RNA Viruses Benefit from Autophagosome Maturation. *J. Virol.* **87**, 9966–9972 (2013).

56. M. Gannagé, D. Dormann, R. Albrecht, J. Dengjel, T. Torossi, P. C. Rämer, M. Lee, T. Strowig, F. Arrey, G. Conenello, M. Pypaert, J. Andersen, A. García-Sastre, C. Münz, Matrix Protein 2 of Influenza A Virus Blocks Autophagosome Fusion with Lysosomes. *Cell Host Microbe.* **6**, 367–380 (2009).

57. Y. Miyanari, K. Atsuzawa, N. Usuda, K. Watashi, T. Hishiki, M. Zayas, R. Bartenschlager, T. Wakita, M. Hijikata, K. Shimotohno, The lipid droplet is an important organelle for hepatitis C virus production. *Nat. Cell Biol.* **9**, 1089–1097 (2007).

58. J. Li, Y. Liu, Z. Wang, K. Liu, Y. Wang, J. Liu, H. Ding, Z. Yuan, Subversion of Cellular Autophagy Machinery by Hepatitis B Virus for Viral Envelopment. *J. Virol.* **85**, 6319–6333 (2011).

59. S. Shoji-Kawata, B. Levine, Autophagy, antiviral immunity, and viral countermeasures. *Biochim. Biophys. Acta - Mol. Cell Res.* **1793** (2009), pp. 1478–1484.

60. M. Kvansakul, S. Caria, M. G. Hinds, The Bcl-2 family in host-virus interactions. *Viruses.* **9** (2017), doi:10.3390/v9100290.

61. M. Chaumorcel, M. Lussignol, L. Mouna, Y. Cavignac, K. Fahie, J. Cotte-Laffitte, A. Geballe, W. Brune, I. Beau, P. Codogno, A. Esclatine, The Human Cytomegalovirus Protein TRS1 Inhibits Autophagy via Its Interaction with Beclin 1. *J. Virol.* **86**, 2571–2584 (2012).

62. A. M. Yakoub, D. Shukla, Autophagy stimulation abrogates herpes simplex virus-1 infection. *Sci. Rep.* **5** (2015), doi:10.1038/srep09730.

63. X. Dong, B. Levine, Autophagy and Viruses: Adversaries or Allies? *J. Innate Immun.* **5**, 480 (2013).

64. J. Mao, E. Lin, L. He, J. Yu, P. Tan, Y. Zhou, Autophagy and Viral Infection. *Autophagy Regul. Innate Immun.* **1209**, 55 (2019).

65. S. Liang, Y. S. Wu, D. Y. Li, J. X. Tang, H. F. Liu, Autophagy in Viral Infection and Pathogenesis. *Front. Cell Dev. Biol.* **9** (2021), doi:10.3389/FCELL.2021.766142.

66. B. R. Wasik, P. E. Turner, On the Biological Success of Viruses. *http://dx.doi.org/10.1146/annurev-micro-090110-102833.* **67**, 519–541 (2013).

67. P. Zhong, L. M. Agosto, J. B. Munro, W. Mothes, Cell-to-cell transmission of viruses. *Curr. Opin. Virol.* **3**, 44 (2013).

68. L. M. Agosto, P. D. Uchil, W. Mothes, HIV cell-to-cell transmission: effects on pathogenesis and antiretroviral therapy. *Trends Microbiol.* **23**, 289 (2015).

69. J. Dufloo, T. Bruel, O. Schwartz, HIV-1 cell-to-cell transmission and broadly neutralizing antibodies. *Retrovirology 2018 151.* **15**, 1–14 (2018).

70. N. Barretto, S. L. Uprichard, Hepatitis C virus Cell-to-cell Spread Assay. *Bio-protocol.* **4** (2014), doi:10.21769/BIOPROTOC.1365.

71. Z. Liu, J. J. He, Cell-Cell Contact-Mediated Hepatitis C Virus (HCV) Transfer, Productive Infection, and Replication and Their Requirement for HCV Receptors. *J. Virol.* **87**, 8545 (2013).

72. J. C. Carmichael, H. Yokota, R. C. Craven, A. Schmitt, J. W. Wills, The HSV-1

mechanisms of cell-to-cell spread and fusion are critically dependent on host PTP1B. *PLOS Pathog.* **14**, e1007054 (2018).

73. S. Bär, A. Takada, Y. Kawaoka, M. Alizon, Detection of Cell-Cell Fusion Mediated by Ebola Virus Glycoproteins. *J. Virol.* **80**, 2815 (2006).

74. D. Walsh, M. H. Naghavi, Exploitation of cytoskeletal networks during early viral infection. *Trends Microbiol.* **27**, 39 (2019).

75. Q. Sattentau, Avoiding the void: cell-to-cell spread of human viruses. *Nat. Rev. Microbiol.* **6**, 815–826 (2008).

76. S. A. Lauer, K. H. Grantz, Q. Bi, F. K. Jones, Q. Zheng, H. R. Meredith, A. S. Azman, N. G. Reich, J. Lessler, The incubation period of coronavirus disease 2019 (CoVID-19) from publicly reported confirmed cases: Estimation and application. *Ann. Intern. Med.* **172**, 577–582 (2020).

77. D. B. Araujo, R. R. G. Machado, D. E. Amgarten, F. de M. Malta, G. G. de Araujo, C. O. Monteiro, E. D. Candido, C. P. Soares, F. G. de Menezes, A. C. C. Pires, R. A. F. Santana, A. de O. Viana, E. Dorlass, L. Thomazelli, L. C. de S. Ferreira, V. F. Botosso, C. R. G. Carvalho, D. B. L. Oliveira, J. R. R. Pinho, E. L. Durigon, SARS-CoV-2 isolation from the first reported patients in brazil and establishment of a coordinated task network. *Mem. Inst. Oswaldo Cruz.* **115**, 1–8 (2020).

78. S. R. Leist, A. Schäfer, D. R. Martinez, Cell and animal models of SARS-CoV-2 pathogenesis and immunity. *DMM Dis. Model. Mech.* **13** (2020), doi:10.1242/dmm.046581.

79. M. Hoffmann, H. Kleine-Weber, S. Schroeder, N. Krüger, T. Herrler, S. Erichsen, T. S. Schiergens, G. Herrler, N. H. Wu, A. Nitsche, M. A. Müller, C. Drosten, S. Pöhlmann, SARS-CoV-2 Cell Entry Depends on ACE2 and TMPRSS2 and Is Blocked by a Clinically Proven Protease Inhibitor. *Cell* (2020), doi:10.1016/j.cell.2020.02.052.

80. E. C. Mossel, C. Huang, K. Narayanan, S. Makino, R. B. Tesh, C. J. Peters, Exogenous ACE2 Expression Allows Refractory Cell Lines To Support Severe Acute Respiratory Syndrome Coronavirus Replication. *J. Virol.* **79**, 3846–3850 (2005).

81. V. Cagno, SARS-CoV-2 cellular tropism. *The Lancet Microbe* (2020), doi:10.1016/s2666-5247(20)30008-2.

82. N. S. Ogando, T. J. Dalebout, J. C. Zevenhoven-Dobbe, R. W. A. L. Limpens, Y. van der Meer, L. Caly, J. Druce, J. J. C. de Vries, M. Kikkert, M. Barcena, I. Sidorov, E. J. Snijder, SARS-coronavirus-2 replication in VERO E6 cells: Replication kinetics, rapid adaptation and cytopathology. *J. Gen. Virol.* (2020), doi:10.1099/jgv.0.001453.

83. K. Takayama, In Vitro and Animal Models for SARS-CoV-2 research. *Trends Pharmacol. Sci.* (2020), , doi:10.1016/j.tips.2020.05.005.

84. I. Glowacka, S. Bertram, P. Herzog, S. Pfefferle, I. Steffen, M. O. Muench, G. Simmons, H. Hofmann, T. Kuri, F. Weber, J. Eichler, C. Drosten, S. Pöhlmann, Differential Downregulation of ACE2 by the Spike Proteins of Severe Acute Respiratory Syndrome Coronavirus and Human Coronavirus NL63. *J. Virol.* **84**, 1198–1205 (2010).

85. N. Z. Cuervo, N. Grandvaux, Ace2: Evidence of role as entry receptor for sars-cov-2 and implications in medical conditions. *Elife.* **9**, 1–25 (2020).

86. Técnica de baixo custo permite ver o novo coronavírus dentro da célula em 3D | AGÊNCIA FAPESP, (available at https://agencia.fapesp.br/tecnica-de-baixo-custo-permite-ver-o-novo-coronavirus-dentro-da-celula-em-3d/33800/).

87. D. A. Nyayanit, P. Sarkale, S. Baradkar, S. Patil, P. D. Yadav, A. Shete-Aich, K. Kalele, P. Gawande, T. Majumdar, R. Jain, G. Sapkal, Transcriptome & viral growth analysis of SARS-CoV-2-infected VERO CCL-81 cells. *Indian J. Med. Res.* **152**, 70–76 (2020).

88. S. Eymieux, Y. Rouillé, O. Terrier, K. Seron, E. Blanchard, M. Rosa-Calatrava, J. Dubuisson, S. Belouzard, P. Roingeard, Ultrastructural modifications induced by SARS-CoV-2 in VERO cells: a kinetic analysis of viral factory formation, viral particle morphogenesis and virion release. *Cell. Mol. Life Sci.* **78**, 3565–3576 (2021).

89. H. Chu, J. F.-W. Chan, T. T.-T. Yuen, H. Shuai, S. Yuan, Y. Wang, B. Hu, C. C.-Y. Yip, J. O.-L. Tsang, X. Huang, Y. Chai, D. Yang, Y. Hou, K. K.-H. Chik, X. Zhang, A. Y.-F. Fung, H.-W. Tsoi, J.-P. Cai, W.-M. Chan, J. D. Ip, A. W.-H. Chu, J. Zhou, D. C. Lung, K.-H. Kok, K. K.-W. To, O. T.-Y. Tsang, K.-H. Chan, K.-Y. Yuen, Comparative tropism, replication kinetics, and cell damage profiling of SARS-CoV-2 and SARS-CoV with implications for clinical manifestations, transmissibility, and laboratory studies of COVID-19: an observational study. *The Lancet Microbe*. **1**, e14–e23 (2020).

90. D. K. Banfield, W. Prinz, *Curr. Opin. Cell Biol.*, in press, doi:10.1016/J.CEB.2014.07.001.

91. M. J. Kennedy, M. D. Ehlers, Organelles and Trafficking Machinery for Postsynaptic Plasticity. *Annu. Rev. Neurosci.* **29**, 325 (2006).

92. N. Naslavsky, S. Caplan, The enigmatic endosome – sorting the ins and outs of endocytic trafficking. *J. Cell Sci.* **131** (2018), doi:10.1242/JCS.216499.

93. Y. B. Hu, E. B. Dammer, R. J. Ren, G. Wang, The endosomal-lysosomal system: From acidification and cargo sorting to neurodegeneration. *Transl. Neurodegener.* **4**, 1–10 (2015).

94. G. Das, B. V. Shravage, E. H. Baehrecke, Regulation and Function of Autophagy during Cell Survival and Cell Death. *Cold Spring Harb. Perspect. Biol.* **4**, 1–14 (2012).

95. D. Stalder, D. C. Gershlick, Direct trafficking pathways from the Golgi apparatus to the plasma membrane. *Semin. Cell Dev. Biol.* **107**, 112 (2020).

96. V. Hyenne, M. Labouesse, J. G. Goetz, The Small GTPase Ral orchestrates MVB biogenesis and exosome secretion. *Small GTPases*. **9**, 445 (2018).

97. C. B. Jones, E. M. Ott, J. M. Keener, M. Curtiss, V. Sandrin, M. Babst, Regulation of Membrane Protein Degradation by Starvation-Response Pathways. *Traffic*. **13**, 468–482 (2012).

98. S. B. Kudchodkar, B. Levine, Viruses and autophagy. *Rev. Med. Virol.* **19** (2009), pp. 359–378.

99. Y. Choi, J. W. Bowman, J. U. Jung, Autophagy during viral infection - A double-edged sword. *Nat. Rev. Microbiol.* **16**, 341–354 (2018).

100. H. Pi, M. Li, L. Tian, Z. Yang, Z. Yu, Z. Zhou, Enhancing lysosomal biogenesis and autophagic flux by activating the transcription factor EB protects against cadmium-induced neurotoxicity. *Sci. Rep.* **7**, 1–14 (2017).

101. J. Saraste, K. Prydz, Assembly and Cellular Exit of Coronaviruses: Hijacking an Unconventional Secretory Pathway from the Pre-Golgi Intermediate Compartment via the Golgi Ribbon to the Extracellular Space. *Cells*. **10** (2021), , doi:10.3390/cells10030503.

102. Y. L. Siu, K. T. Teoh, J. Lo, C. M. Chan, F. Kien, N. Escriou, S. W. Tsao, J. M. Nicholls, R. Altmeyer, J. S. M. Peiris, R. Bruzzone, B. Nal, The M, E, and N Structural Proteins of the Severe Acute Respiratory Syndrome Coronavirus Are

Required for Efficient Assembly, Trafficking, and Release of Virus-Like Particles. *J. Virol.* **82**, 11318–11330 (2008).

103. R. Pierini, E. Cottam, R. Roberts, T. Wileman, Modulation of membrane traffic between endoplasmic reticulum, ERGIC and Golgi to generate compartments for the replication of bacteria and viruses. *Semin. Cell Dev. Biol.* **20** (2009), pp. 828–833.

104. M. C. Hagemeijer, M. H. Verheije, M. Ulasli, I. A. Shaltiël, L. A. de Vries, F. Reggiori, P. J. M. Rottier, C. A. M. de Haan, Dynamics of Coronavirus Replication-Transcription Complexes. *J. Virol.* **84**, 2134–2149 (2010).

105. E. J. Snijder, R. W. A. L. Limpens, A. H. de Wilde, A. W. M. de Jong, J. C. Zevenhoven-Dobbe, H. J. Maier, F. F. G. A. Faas, A. J. Koster, M. Bárcena, A unifying structural and functional model of the coronavirus replication organelle: Tracking down RNA synthesis. *PLoS Biol.* **18**, e3000715 (2020).

106. A. Reggio, V. Buonomo, P. Grumati, Eating the unknown: Xenophagy and ER-phagy are cytoprotective defenses against pathogens. *Exp. Cell Res.* **396** (2020), , doi:10.1016/j.yexcr.2020.112276.

107. S. Klein, M. Cortese, S. L. Winter, M. Wachsmuth-Melm, C. J. Neufeldt, B. Cerikan, M. L. Stanifer, S. Boulant, R. Bartenschlager, P. Chlanda, SARS-CoV-2 structure and replication characterized by in situ cryo-electron tomography. *Nat. Commun.* **11**, 1–10 (2020).

108. N. Cifuentes-Muñoz, R. E. Dutch, R. Cattaneo, Direct cell-to-cell transmission of respiratory viruses: The fast lanes. *PLOS Pathog.* **14**, e1007015 (2018).

109. P. Zhong, L. M. Agosto, J. B. Munro, W. Mothes, Cell-to-cell transmission of viruses. *Curr. Opin. Virol.* **3**, 44 (2013).

110. Q. Sattentau, Avoiding the void: cell-to-cell spread of human viruses. *Nat. Rev. Microbiol. 2008 611*. **6**, 815–826 (2008).

111. C. Zeng, J. P. Evans, T. King, Y. M. Zheng, E. M. Oltz, S. P. J. Whelan, L. J. Saif, M. E. Peeples, S. L. Liu, SARS-CoV-2 spreads through cell-to-cell transmission. *Proc. Natl. Acad. Sci. U. S. A.* **119**, e2111400119 (2022).

112. A. Pepe, S. Pietropaoli, M. Vos, G. Barba-Spaeth, C. Zurzolo, Tunneling nanotubes provide a route for SARS-CoV-2 spreading. *Sci. Adv.* **8**, 171 (2022).

113. V. Sharma, S. Verma, E. Seranova, S. Sarkar, D. Kumar, Selective autophagy and xenophagy in infection and disease. *Front. Cell Dev. Biol.* **6** (2018), p. 147.

114. W. T. Jackson, Viruses and the autophagy pathway. *Virology.* **479–480** (2015), pp. 450–456.

115. J. Mao, E. Lin, L. He, J. Yu, P. Tan, Y. Zhou, in *Advances in Experimental Medicine and Biology* (Springer, 2019; https://doi.org/10.1007/978-981-15-0606-2_5), vol. 1209, pp. 55–78.

116. M. Marsh, in *Endosomes* (Springer New York, 2008; https://link.springer.com/chapter/10.1007/978-0-387-39951-5_11), pp. 132–144.

117. W. Sun, Ambra1 in autophagy and apoptosis: Implications for cell survival and chemotherapy resistance (Review). *Oncol. Lett.* **12**, 367–374 (2016).

118. N. J. Lennemann, C. B. Coyne, R. C. Condit, Ed., Catch Me If You Can: The Link between Autophagy and Viruses. *PLoS Pathog.* **11** (2015), pp. 1–6.

119. Y. Wang, L. Li, C. Hou, Y. Lai, J. Long, J. Liu, Q. Zhong, J. Diao, SNARE-mediated membrane fusion in autophagy. *Semin. Cell Dev. Biol.* **60**, 97 (2016).

120. J. Kale, E. J. Osterlund, D. W. Andrews, BCL-2 family proteins: changing partners in the dance towards death. *Nat. Publ. Gr.* **25**, 65–80 (2017).

121. B. F, B. R, M. T, E. M. F, P. HW, Regulation of the Tumor-Suppressor BECLIN

1 by Distinct Ubiquitination Cascades. *Int. J. Mol. Sci.* **18** (2017), doi:10.3390/IJMS18122541.

122. J.-P. Decuypere, J. B. Parys, G. Bultynck, Regulation of the Autophagic Bcl-2/Beclin 1 Interaction. *Cells* (2012), doi:10.3390/cells1030284.

123. L. C. Jones, L. Moussa, M. L. Fulcher, Y. Zhu, E. J. Hudson, W. K. O'Neal, S. H. Randell, E. R. Lazarowski, R. C. Boucher, S. M. Kreda, VAMP8 is a vesicle SNARE that regulates mucin secretion in airway goblet cells. *J. Physiol.* **590**, 545 (2012).

124. W. CC, N. CP, L. L, A. V, Z. W, S. LF, H. W, A role of VAMP8/endobrevin in regulated exocytosis of pancreatic acinar cells. *Dev. Cell.* **7**, 359–371 (2004).

125. W. CC, S. H, G. K, N. CP, L. J, G. BQ, C. L. H, L. J, R. H, Z. ZH, Z. Q, H. W, VAMP8/endobrevin as a general vesicular SNARE for regulated exocytosis of the exocrine system. *Mol. Biol. Cell.* **18**, 1056–1063 (2007).

126. Q. Ren, H. K. Barber, G. L. Crawford, Z. A. Karim, C. Zhao, W. Choi, C.-C. Wang, W. Hong, S. W. Whiteheart, Endobrevin/VAMP-8 Is the Primary v-SNARE for the Platelet Release Reaction. *Mol. Biol. Cell.* **18**, 24 (2007).

127. P. PN, T. HK, W. CC, H. W, M. AJ, VAMP8 is essential in anaphylatoxin-induced degranulation, TNF-alpha secretion, peritonitis, and systemic inflammation. *J. Immunol.* **183**, 1413–1418 (2009).

128. T. N, W. CC, B. C, K. G, V. F, Q. Z, R. J, S. MR, Z. G, H. W, B. U, VAMP-8 segregates mast cell-preformed mediator exocytosis from cytokine trafficking pathways. *Blood.* **111**, 3665–3674 (2008).

129. W. Antonin, C. Holroyd, R. Tikkanen, S. Honing, R. Jahn, The R-SNARE endobrevin/VAMP-8 mediates homotypic fusion of early endosomes and late endosomes. *Mol. Biol. Cell* (2000), doi:10.1091/mbc.11.10.3289.

130. M. R. Marshall, V. Pattu, M. Halimani, M. Maier-Peuschel, M. L. Müller, U. Becherer, W. Hong, M. Hoth, T. Tschernig, Y. T. Bryceson, J. Rettig, VAMP8-dependent fusion of recycling endosomes with the plasma membrane facilitates T lymphocyte cytotoxicity. *J. Cell Biol.* (2015), doi:10.1083/jcb.201411093.

131. S. Malmersjö, S. Di Palma, J. Diao, Y. Lai, R. A. Pfuetzner, A. L. Wang, M. A. McMahon, A. Hayer, M. Porteus, B. Bodenmiller, A. T. Brunger, T. Meyer, Phosphorylation of residues inside the SNARE complex suppresses secretory vesicle fusion . *EMBO J.* **35**, 1810–1821 (2016).

132. E. Keyaerts, L. Vijgen, P. Maes, J. Neyts, M. Van Ranst, Growth kinetics of SARS-coronavirus in VERO E6 cells. *Biochem. Biophys. Res. Commun.* **329**, 1147–1151 (2005).

133. M. Camacho, J. D. Machado, J. Alvarez, R. Borges, Intravesicular calcium release mediates the motion and exocytosis of secretory organelles: A study with adrenal chromaffin cells. *J. Biol. Chem.* **283**, 22383–22389 (2008).

134. M. J. Vincent, E. Bergeron, S. Benjannet, B. R. Erickson, P. E. Rollin, T. G. Ksiazek, N. G. Seidah, S. T. Nichol, Chloroquine is a potent inhibitor of SARS coronavirus infection and spread. *Virol. J.* **2**, 69 (2005).

135. E. Keyaerts, S. Li, L. Vijgen, E. Rysman, J. Verbeeck, M. Van Ranst, P. Maes, Antiviral activity of chloroquine against human coronavirus OC43 infection in newborn mice. *Antimicrob. Agents Chemother.* **53**, 3416–3421 (2009).

136. E. Keyaerts, L. Vijgen, P. Maes, J. Neyts, M. Van Ranst, In vitro inhibition of severe acute respiratory syndrome coronavirus by chloroquine. *Biochem. Biophys. Res. Commun.* **323**, 264–268 (2004).

137. M. Kono, K. Tatsumi, A. M. Imai, K. Saito, T. Kuriyama, H. Shirasawa,

Inhibition of human coronavirus 229E infection in human epithelial lung cells (L132) by chloroquine: Involvement of p38 MAPK and ERK. *Antiviral Res.* **77**, 150–152 (2008).

138. B. Jia, Y. Xue, X. Yan, J. Li, Y. Wu, R. Guo, J. Zhang, L. Zhang, Y. Li, Y. Liu, L. Sun, Autophagy inhibitor chloroquine induces apoptosis of cholangiocarcinoma cells via endoplasmic reticulum stress. *Oncol. Lett.* **16**, 3509–3516 (2018).

139. M. Hoffmann, K. Mösbauer, H. Hofmann-Winkler, A. Kaul, H. Kleine-Weber, N. Krüger, N. C. Gassen, M. A. Müller, C. Drosten, S. Pöhlmann, Chloroquine does not inhibit infection of human lung cells with SARS-CoV-2. *Nat. 2020 5857826.* **585**, 588–590 (2020).

140. M. Mauthe, I. Orhon, C. Rocchi, X. Zhou, M. Luhr, K. J. Hijlkema, R. P. Coppes, N. Engedal, M. Mari, F. Reggiori, Chloroquine inhibits autophagic flux by decreasing autophagosome-lysosome fusion. *Autophagy.* **14**, 1435–1455 (2018).

141. T. Ou, H. Mou, L. Zhang, A. Ojha, H. Choe, M. Farzan, Hydroxychloroquine-mediated inhibition of SARS-CoV-2 entry is attenuated by TMPRSS2. *PLOS Pathog.* **17**, e1009212 (2021).

142. C. Q. Sacramento, N. Fintelman-Rodrigues, S. S. G. Dias, J. R. Temerozo, A. De, P. D. Da Silva, C. S. Da Silva, A. C. Ferreira, M. Mattos, V. C. Soares, F. Pereira-Dutra, M. D. Miranda, D. F. Barreto-Vieira, M. Alexandre, N. Da Silva, S. S. Santos, M. Torres, R. K. R. Rajoli, A. Paccanaro, A. Owen, D. Chequer Bou-Habib, P. T. Bozza, T. Moreno, L. Souza, Title: Unlike Chloroquine, mefloquine inhibits SARS-CoV-2 infection in physiologically relevant cells and does not induce viral variants Short title: SARS-CoV-2 is susceptible to mefloquine in type II pneumocytes and monocytes, doi:10.1101/2021.07.21.451321.

143. O. Kapuy, T. Korcsmáros, Chloroquine and COVID-19—A systems biology model uncovers the drug's detrimental effect on autophagy and explains its failure. *PLoS One.* **17**, e0266337 (2022).

144. P. J. Mullen, G. Garcia, A. Purkayastha, N. Matulionis, E. W. Schmid, M. Momcilovic, C. Sen, J. Langerman, A. Ramaiah, D. B. Shackelford, R. Damoiseaux, S. W. French, K. Plath, B. N. Gomperts, V. Arumugaswami, H. R. Christofk, SARS-CoV-2 infection rewires host cell metabolism and is potentially susceptible to mTORC1 inhibition. *Nat. Commun. 2021 121.* **12**, 1–10 (2021).

145. É. P. Zambalde, T. L. Dias, G. C. Maktura, M. R. Amorim, B. Brenha, L. N. Santos, L. Buscaratti, J. G. de A. Elston, M. C. S. Mancini, I. C. B. Pavan, D. A. Toledo-Teixeira, K. Bispo-dos-Santos, P. L. Parise, A. P. Morelli, L. G. S. da Silva, Í. M. S. de Castro, T. D. Saccon, M. A. Mori, F. Granja, H. I. Nakaya, J. L. Proenca-Modena, H. Marques-Souza, F. M. Simabuco, Increased mTOR Signaling and Impaired Autophagic Flux Are Hallmarks of SARS-CoV-2 Infection. *Curr. Issues Mol. Biol.* **45**, 327–336 (2023).

ATTACHMENTS

Declaration that the work did not involve research with human beings, animals, genetic heritage, or topics related to biosafety.

COORDENADORIA DE PÓS-GRADUAÇÃO
INSTITUTO DE BIOLOGIA
Universidade Estadual de Campinas
Caixa Postal 6109. 13083-970, Campinas, SP, Brasil
Fone (19) 3521-6378. email: cpgib@unicamp.br

UNICAMP

IB

DECLARAÇÃO

Em observância ao **§5º do Artigo 1º da Informação CCPG-UNICAMP/001/15**, referente a Bioética e Biossegurança, declaro que o conteúdo de minha Dissertação de Mestrado, intitulada "*SARS-CoV-2 UTILIZES INCOMPLETE AUTOPHAGY FLUX TO PROMOTE VIRAL REPLICATION AND CELL-TO-CELL CONNECTIONS TO PROMOTE CELLULAR EVASION*", desenvolvida no Programa de Pós-Graduação em Biologia Molecular e Morfofuncional do Instituto de Biologia da Unicamp, não versa sobre pesquisa envolvendo seres humanos, animais ou temas afetos a Biossegurança.

Assinatura: _____
Nome do(a) aluno(a): GRAZIELLE CELESTE MAKTURA

Assinatura: _____
Nome do(a) orientador(a): HENRIQUE MARQUES BARBOSA DE SOUZA
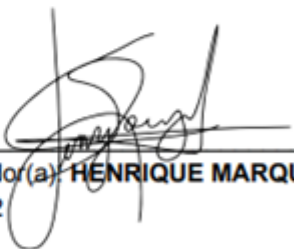
Data: 28/07/2023

Declaration that the dissertation or thesis does not infringe the provisions of law nº 9610/98, nor the copyright of any publisher.

Declaração

As cópias de artigos de minha autoria ou de minha co-autoria, já publicados ou submetidos para publicação em revistas científicas ou anais de congressos sujeitos a arbitragem, que constam da minha Dissertação/Tese de Mestrado/Doutorado, intitulada **SARS-CoV-2 UTILIZES INCOMPLETE AUTOPHAGY FLUX TO PROMOTE VIRAL REPLICATION AND CELL-TO-CELL CONNECTIONS TO PROMOTE CELLULAR EVASION**, não infringem os dispositivos da Lei n.° 9.610/98, nem o direito autoral de qualquer editora.

Campinas, 28/07/2023

Assinatura : _____

Nome do(a) autor(a): **GRAZIELLE CELESTE MAKTURA**

RG n.° 52.884.916-5

Assinatura : _____

Nome do(a) orientador(a): **HENRIQUE MARQUES BARBOSA DE SOUZA**

RG n.° 66.253.888-2